

S. Hagemann · B. Machenhauer · R. Jones
O. B. Christensen · M. Déqué · D. Jacob · P. L. Vidale

Evaluation of water and energy budgets in regional climate models applied over Europe

Received: 14 November 2003 / Accepted: 14 April 2004 / Published online: 7 August 2004
© Springer-Verlag 2004

Abstract This study presents a model intercomparison of four regional climate models (RCMs) and one variable resolution atmospheric general circulation model (AGCM) applied over Europe with special focus on the hydrological cycle and the surface energy budget. The models simulated the 15 years from 1979 to 1993 by using quasi-observed boundary conditions derived from ECMWF re-analyses (ERA). The model intercomparison focuses on two large catchments representing two different climate conditions covering two areas of major research interest within Europe. The first is the Danube catchment which represents a continental climate dominated by advection from the surrounding land areas. It is used to analyse the common model error of a too dry and too warm simulation of the summertime climate of southeastern Europe. This summer warming and drying problem is seen in many RCMs, and to a less extent in GCMs. The second area is the Baltic Sea catchment which represents maritime climate dominated by advection from the ocean and from the Baltic Sea. This catchment is a research area of many studies within Europe and also covered by the BALTEX program. The observed data used are monthly mean surface air tem-

perature, precipitation and river discharge. For all models, these are used to estimate mean monthly biases of all components of the hydrological cycle over land. In addition, the mean monthly deviations of the surface energy fluxes from ERA data are computed. Atmospheric moisture fluxes from ERA are compared with those of one model to provide an independent estimate of the convergence bias derived from the observed data. These help to add weight to some of the inferred estimates and explain some of the discrepancies between them. An evaluation of these biases and deviations suggests possible sources of error in each of the models. For the Danube catchment, systematic errors in the dynamics cause the prominent summer drying problem for three of the RCMs, while for the fourth RCM this is related to deficiencies in the land surface parametrization. The AGCM does not show this drying problem. For the Baltic Sea catchment, all models similarly overestimate the precipitation throughout the year except during the summer. This model deficit is probably caused by the internal model parametrizations, such as the large-scale condensation and the convection schemes.

S. Hagemann (✉) · D. Jacob
Max Planck Institute for Meteorology, Bundesstraße 55,
20146 Hamburg, Germany
E-mail: hagemann@dkrz.de

R. Jones
Meteorological Office Hadley Centre, London Road, Bracknell,
RG12 2SY, UK

B. Machenhauer · O. B. Christensen
Climate Research Division, Danish Meteorological Institute,
Lyngbyvej 100, Copenhagen Ø, 2100, Denmark

M. Déqué
Météo-France CNRM/GMGEC/EAC, 42 Avenue Coriolis,
Toulouse Cedex 01, 31057, France

P. L. Vidale
Climate Research ETH, Winterthurerstrasse 190,
Zürich, 8057, Switzerland

1 Introduction

The EU project MERCURE (Modelling European Regional Climate: Understanding and Reducing Errors) was launched to improve regional climate models by understanding and reducing sources of errors, notably those arising through poor parametrization of physical processes and insufficient model resolution. Several European partners have participated with their regional climate models (RCMs) in the MERCURE project. The HIRHAM4 high resolution limited area model (Christensen et al. 1996) was used by two of the partners, DMI (Danish Meteorological Institute) and MPI (Max-Planck-Institute for Meteorology). Here, a close, long-

lasting cooperation between DMI and MPI in EU supported regionalization projects (Machenhauer et al. 1996, 1998) was continued. The ARPEGE model (Déqué et al. 1998) was used by Météo-France, a modified version of the German Weather Service's forecast Europa model (CHRM; Lüthi et al. 1996) was used by the Institute for Climate Research of the ETH Zurich, and the HadRM3H model (Jones et al. 1995) was used by the Hadley Centre.

This study presents a model intercomparison of the models that have participated in the MERCURE project plus the REMO model developed at MPI (Jacob 2001) with a special focus on the hydrological cycle and the surface energy budget. Involving the REMO model in the study adds an interesting dimension as it shares the dynamical core of the CHRM model and the physics of the HIRHAM model. A total of 15 years of model simulations covering the time from 1979 to 1993 and conducted at roughly 50 km resolution were compared. To minimize the influence of errors in the prescribed SSTs and the lateral boundary conditions, these were determined from ECMWF re-analysis data (ERA; Gibson et al. 1997) for all models except for the ARPEGE model which used only prescribed SSTs as it is a global model using a stretched model grid with a high resolution over Europe (see Sect. 2.2). Here, ARPEGE uses the monthly reconstructed SST dataset ("Reynolds SSTs") of NCEP (Smith et al. 1996). No spin-up period was simulated by the models except for ARPEGE where the simulation started in 1960. HIRHAM has simulated the first year 1979 twice, thereby initializing the soil variables of the main simulation at 1 January 1979 with the soil variables from 30 December 1979 of the first simulation. With regards to soil moisture and temperature REMO was initialized with ERA data, CHRM with a typical state based on previous simulations using ERA and HadRM3H with a typical state based on previous simulations driven by a GCM. Note that an evaluation of the same model simulations used in the present study with respect to daily precipitation statistics over the Alps is given by Frei et al. (2003). In addition, Vidale et al. (2003) focused on the interannual variability (temperature, precipitation and energy fluxes) of the CHRM simulation over eight European sub-domains.

For the model intercomparison two large European catchments were chosen which represent two different climate conditions. The Danube catchment represents continental climate as it is land-dominated by advection from the surrounding land areas, the Baltic Sea catchment represents maritime climate since it is water-dominated by advection from the ocean and from the Baltic Sea. It is of interest to see whether the model behaviour and their systematic errors are similar for both climate regions and how differently the model respond to the systematic errors.

Previous analysis of some of the models has shown that common systematic errors in the RCMs and their driving GCMs can explain some of the biases in the two m-temperature and the precipitation (Machenhauer

et al. 1996, 1998). A special model feature that is typical for many RCMs, and to a less extent is visible in some GCMs, is the too dry and too warm simulation of climate over southeastern Europe during the summer (Machenhauer et al. 1998). These studies showed that this bias could not be explained by systematic errors in the large scale general circulation. Thus, one major task in MERCURE was to understand and reduce or eliminate this model error referred to as the summer drying problem in the following. Hence, this study focuses on the Danube catchment, a large drainage basin contained in the area where this problem occurs.

The second focus of this study is the Baltic Sea catchment which is an area of high research interest within Europe aiming to intending to understand and describe its climate and the components of the water and energy budgets (e.g., see Bengtsson 2001). This area is also covered by the Baltic Sea Experiment (BALTEX) (see BALTEX 1995) which is a European sub-program of the 'Global Energy and Water Cycle Experiment' (GEWEX; WMO 1988).

Section 2 gives a short overview of the participating RCMs. In Sect. 3, the methods are described that were used to compute the water and energy balances at the land surface and the biases in the hydrological cycle. Section 4 focuses on the Danube catchment and Sect. 5 on the Baltic Sea catchment.

2 The regional climate models

Table 1 summarizes the grid configurations, domain characteristics and parametrizations of the RCMs. Other aspects of the RCMs are shortly described in the following sections. Note that the dynamics of the global model ARPEGE are close to the ERA model, as well as the radiative code. The latter applies also to HIRHAM and REMO. All models are more or less simulating the domain shown in Fig. 1. For a detailed definition, see Table 1.

2.1 HIRHAM

The regional climate model HIRHAM4 (Christensen et al. 1996) is based on the HIRLAM (HIgh Resolution Limited Area Model) short-range weather prediction model (Källén 1996). In order to make a model that is suitable for long climate integrations with lateral boundary conditions taken from the MPI global climate model ECHAM4 (Roeckner et al. 1996), the physical parametrization of the ECHAM4 model has been incorporated into the regional model. HIRHAM4 is a standard Eulerian primitive-equation staggered grid point model with additionally a prognostic cloud water equation (as in ECHAM4). A linear fourth-order horizontal diffusion scheme is applied, but in mountainous regions it is switched off for temperature and humidity in order to avoid spurious mixing of air masses from dif-

Table 1 Summary of grid configurations and parameterizations for the RCMs

| | HIRHAM | ARPEGE | CHRM | HadRM3H | REMO |
|---------------------------|---|---|---|--|--|
| Grid resolution | 0.44° (50 km) | 50–70 km (over Europe) | 0.5° (55 km) | 0.44° (50 km) | 0.5° (50 km) |
| Grid (latitude*longitude) | 110 × 104 | see Sect. 2.2 | 81 × 91 | 106 × 111 | 81 × 91 |
| South pole | 27°E, 37°S | see Sect. 2.2 | 10°E, 32.5°S | 10°E, 38°S | 10°E, 32.5°S |
| Vertical levels | 19 | 31 | 20 | 19 | 20 |
| Lateral boundary | Davies, (1976) | – | Davies, (1976) | – | Davies, (1976) |
| Number of points | 10 | – | 8 | 4 | 8 |
| Convention | Mass flux Tiedtke (1989) | Mass flux Bougeault (1985) | Mass flux Tiedtke (1989) | Mass flux Gregory and Rowntree (1990) | Mass flux Tiedtke (1989) |
| Microphysics | Nordeng 1994 Sundqvist (1988) Ricard and Royer (1993) | Statistical and diagnostic Lin et al. (1983) | Kessler (1969) Jones et al. (1995) | Gregory and Allen (1991) Smith (1990) | Nordeng 1994 for CAPEclosure Sundqvist (1978) |
| Radiation | Morcrette (1991) Giorgetta and Wild (1995) | Morcrette (1990) | Ritter and Geleyn (1992) | Giorgetta and Wild (1995) | Edwards and Slingo (1996) |
| Land surface | Dümenil and Todini (1992) | Douville et al. (2000) | Dickinson (1984) Jacobsen and Heise (1982) | Cox et al. (1999) | Dümenil and Todini (1992) |
| Soil thermal layers | 5 | 4 | 2 | 4 | 5 |
| Soil moisture layers | 1 | 2 | 3 | 4 | 1 |

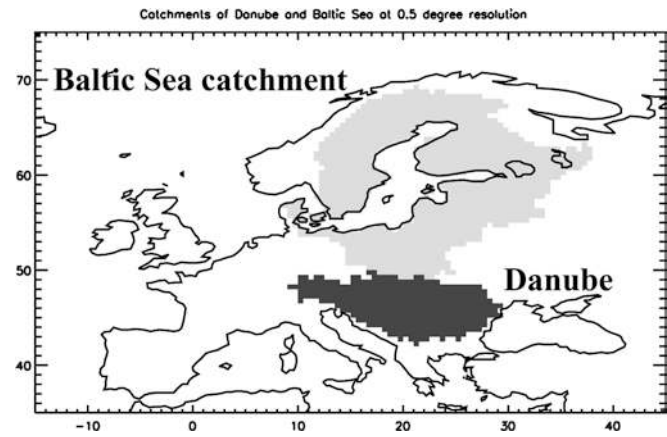


Fig. 1 Catchments of Danube and Baltic Sea at 0.5 degree resolution

ferent levels causing unphysical precipitation. Several changes were made to the HIRHAM4 model presented by Christensen et al. (1996) during the MERCURE project which are described in Hagemann et al. (2001). Moreover, the updated model utilizes high-resolution datasets of land surface characteristics based upon major ecosystem types (Hagemann et al. 1999, Hagemann 2002) and orography (Christensen et al. 2001).

2.2 ARPEGE

The ARPEGE-IFS model is a global atmosphere model developed by the French Meteorological Service Météo-France and the European Centre for Medium-range Weather Forecasts (ECMWF) for operational short- and medium-range forecasting. A climate version of this model was developed at Météo-France (Déqué et al. 1998). This version uses a spectral T106 truncation. The associated grid has 120 pseudo-latitudes and 240 pseudo-longitudes. The pole of the new system of coordinates is located in the Mediterranean Sea. The equations are discretized on an isotropic grid. The antipode is located in the southern Pacific Ocean. A stretching factor is applied as a function of the pseudo-latitude. The maximum value is 3 at the Mediterranean pole, the minimum is 1/3 at the opposite pole. Thus the resolution over Europe is between 50 and 70 km. The physical parametrizations have no strong originality: radiation including indirect effect of aerosols, convection by a mass flux scheme with moisture convergence closure, gravity wave drag with resonance, block, and lift effect, soil processes including a parametrization of the snow age. The cloud-precipitation-vertical diffusion scheme uses a simple turbulent scheme to diagnose the probability distribution of water inside the model mesh.

2.3 CHRM

The Climate High Resolution Model (CHRM, Vidale et al. 2003) is fundamentally a climate version of the

operational mesoscale weather forecasting model of the German and Swiss meteorological services, the HRM (High Resolution Model), previously known as EM (Europa Modell, Majewski and Schrodin 1994, Lüthi et al. 1996). The model has full package of physical parametrizations (see Table 1). The state of the vegetation at the land surface, as described by LAI, roughness and fraction of green vegetation is specified in time and space by assimilating data from the ISLSCP CD-ROM (Sellers et al. 1994), with a spatial resolution of 1 degree and a time resolution of 1 month.

2.4 HadRM3H

HadRM3H is the limited-area higher resolution version of the AGCM HadAM3H which itself is an improved version of HadAM3, the atmospheric component of the latest Hadley Centre coupled AOGCM, HadCM3. HadAM3 is described in Pope et al. (2000), the modifications introduced to form HadAM3H are described in Murphy et al. (in preparation 2002). HadRM3H then uses an identical formulation to HadAM3H except where explicit account must be taken of the impact of higher resolution on the representation of physical and dynamical processes. Changes have been made to the parametrization of the threshold relative humidity for cloud formation to allow for the fact that at higher horizontal resolution more of the spectrum of atmospheric motions are resolved and that the relationship between the variability of humidity at and below the grid scale changes. Also, due to the change in precipitation intensities seen at higher resolution the fractional area of the gridbox over which this is assumed to fall is further changed. One other difference is that the version of HadRM3H used here does not include the sulfur cycle as no relevant lateral boundary data is available consistent with the ERA data used for the meteorological boundary conditions. In this case, a constant (in space and time) average aerosol concentration is assumed.

2.5 REMO

The regional climate model REMO (Vs. 5.0; Jacob 2001) is based on the Europamodell/Deutschlandmodell system (Majewski and Schrodin 1994). REMO may use two different physical parametrization schemes - the original one called DWD-physics or the ECHAM4-physics from the MPI global climate model ECHAM4 (Roeckner et al. 1996) which was used in this study. The dynamical scheme is in both cases identical. A linear fourth-order horizontal diffusion scheme is applied to momentum, temperature and water content. A leap-frog time stepping with semi-implicit correction and Asselin-filter is used. The land surface parametrization scheme in REMO is the same as for HIRHAM (see Sect. 2.1) except for the fact that the land surface parameters fields used in the surface scheme are only based upon Hage-

mann et al. (1999), and the orographic roughness length is computed using a method of Heise (personal communication 2000).

3 Estimation of biases in the water and energy balance

In order to estimate the biases of the components of the simulated hydrological cycle, the corresponding observed values have to be known. The water balance at the land surface is described by

$$P - E - R = \Delta WS = \frac{\Delta W + \Delta S}{\Delta t} \quad (1)$$

P is precipitation, E is evapotranspiration, R is the total runoff occurring at the land surface and ΔWS is the change in the water storage of the soil moisture reservoir ΔW and the accumulated snowpack ΔS within a certain time period Δt . In this study, monthly values will be considered so that $\Delta t = 1$ month. An observed precipitation P_{obs} can be taken from the CRU precipitation dataset (Hulme et al. 1995). But the other components of Eq. (1) are usually not available as observations. Thus, these values have to be estimated.

The total runoff is closely connected to the river discharge for which observed values are commonly available for many catchments. In hydrology, rainfall-runoff models are often used to derive the discharge of a catchment from time series of precipitation. These models are catchment-related and require long time series (usually daily values) of observed precipitation and discharge for their calibration. However, adequate observations are not available for many catchments, so we have developed an estimation approach that does not require the availability of these kind of observations. As observed monthly discharge data are commonly available for many rivers we wanted to find a way to estimate the “observed” total runoff from observed monthly values of discharge.

In Appendix 1, the methodology by which monthly “observed” runoff values R_{obs} are estimated from observed river discharges is described and discussed. For the estimation of the monthly observed storage changes ΔWS_{obs} from the observed precipitation, a similar statistical method was chosen as for the runoff (see also Appendix 1). In this way, a quasi-observed evapotranspiration E_{obs} was estimated by inserting P_{obs} , R_{obs} and ΔWS_{obs} into Eq. (1).

Since in particular the derivation of the statistical relation of δWS_{obs} from P_{obs} is dependent on the realism of the model used for its derivation and it is easily computed for other models than the HIRHAM model we have computed ΔWS_{obs} values from each of the models included in the intercomparison. In the following the estimated bias of the evapotranspiration is called $Bias(E)$ if the statistical relation for ΔWS_{obs} is determined from the model in question whereas it is called $Bias(EQ)$ if this is determined from the HIRHAM model.

Table 2 shows the annual mean values of ΔWS_{obs} and E_{obs} for the Danube and the Baltic Sea catchment. E_{obs} is compared with the ERA evapotranspiration and the observed evapotranspiration calculated by P_{obs} minus the observed discharge following Eq. (1) where the observed ΔWS_{obs} is assumed to be zero in the long-term mean. The annual mean estimates of ΔWS_{obs} do not show large deviations from zero indicating some robustness of these estimates. Here, the annual mean estimates of E_{obs} are close to the observed evapotranspiration whereas the ERA evapotranspiration is overestimated for both catchments, which provides some confidence in the E_{obs} estimates.

Rubel and Hantel (2001) found that over the Baltic Sea catchment it is necessary to correct the observed precipitation data used in this study (see Sect. 5.1). If a corrected annual precipitation amount (+13%) is used to calculate the observed evapotranspiration over the Baltic Sea catchment (35 mm/month), the E_{obs} estimates turn out to be too low. Thus, E_{obs} and the ERA evapotranspiration represent lower and upper bounds for the observed evapotranspiration. Consequently we shall also consider deviations of model evapotranspiration from the ERA evapotranspiration. We call such deviations $Bias(ER)$. It is likely that the actual evapotranspiration bias is just in the middle between $Bias(E)$, $Bias(EQ)$ and $Bias(ER)$.

In general, the monthly means of E_{obs} are relatively similar (not shown), although they vary somewhat in the absolute values. The only exception is E_{obs} based on the ARPEGE simulation which from November–March has a general shape that does not agree with the other four estimates and the ERA evapotranspiration. This seems to be most likely caused by the large overestimation of the accumulated snowpack by ARPEGE which worsens the estimate of ΔWS_{obs} . In April, the textit E_{obs} estimates for the Baltic Sea catchment based on ARPEGE, HIRHAM and HadRM3H are probably unrealistic as they are largely negative.

For an atmospheric column, the water balance is expressed by

$$E - p + C = \frac{\Delta Q}{\Delta t} \quad (2)$$

C is the lateral convergence (divergence if C is negative) of moisture into the column, and $\Delta Q/\Delta t$ is the change of atmospheric moisture content (precipitable water) in the column within a time period Δt (here one month). It

is assumed that the bias in this change from month to month is negligible compared to the biases of the other variables in Eq. (2). The deviation of the different simulated monthly changes in precipitable water from ERA data are small compared to the computed biases in P and E so that the assumption seems to be justified. Thus, Eq. (3) becomes valid for the biases.

$$Bias(C) = Bias(P) - Bias(E) \quad (3)$$

When $Bias(EQ)$ or $Bias(CR)$ are used in this balance instead of $Bias(E)$ the corresponding convergence biases are called $Bias(CQ)$ and $Bias(CR)$, respectively.

It can be assumed that the E estimate is residual from measured P , inferred runoff (from measured discharge) and inferred ΔWS (from measured P). The estimated convergence bias is residual from the P bias and the estimated E bias, and thus the convergence bias can be written as a function of the bias in estimated runoff and water store (hence a function of discharge and P). Also, in the case of the observed evaporation being underestimated (as discussed in Appendix 1 when the model water-store changes are unrealistically low) then negative evaporation biases will tend to be underestimated and so convergence biases less positive or more negative than in reality. Note that one can get a direct C estimate from ERA data over the region by performing an assimilation experiment. It was not possible to obtain a direct C estimate by vertical integration of the lateral atmospheric moisture flows in and out of a region from the archived six-hourly ERA data as the convergence fluxes in the atmosphere are highly non-linear with time.

For the energy balance, appropriate catchment scale observations were not available at the time of the study. Thus, deviations of the simulated energy fluxes from ERA data are computed instead. One has to bear in mind that these data are also some kind of model data following the land surface scheme of Viterbo and Beljaars (1995), although influenced more or less by the available observations in the ERA data-assimilation system. For longer time periods (such as a year), the energy balance at the land surface can be expressed by

$$LHF + SHF + SR + TR = 0 \quad (4)$$

LHF is the latent heat flux, SHF is the sensible heat flux, SR is the surface solar radiation and TR is the surface thermal radiation. All fluxes are positive downward and negative upward.

Table 2 Annual mean of observed estimates for the Danube and the Baltic Sea catchment. Unit: mm/month

| Hydrological variable | HIRHAM | ARPEGE | CHRM | HadRM3H | REMO | ERA | Observed |
|-----------------------|--------|--------|------|---------|------|-----|----------|
| Danube | | | | | | | |
| Evapotranspiration | 45 | 44 | 43 | 44 | 44 | 50 | 44 |
| ΔWS | -1 | 0 | 1 | 0 | 0 | - | 0 |
| Baltic Sea | | | | | | | |
| Evapotranspiration | 27 | 30 | 27 | 29 | 27 | 41 | 28 |
| ΔWS | 1 | -1 | 1 | -1 | 2 | - | 0 |

4 The Danube catchment

The location of the Danube catchment is shown in Fig. 1. Its area comprises about 8,07,000 km² and an annual mean discharge of 6435 m³ /s (203 km³ /a) is observed at a measurement station near the mouth of the river. All the atmospheric variables were integrated over the whole catchment area. Thus, in the following, all the water fluxes will be expressed in mm/month instead of a volume flux unit. As the problems showing up over the Danube catchment are relatively complex and behave differently in each model, the biases in the water balances and the deviations from ERA data in the energy balance are analyzed separately in Sect. 4.2 after the different simulated variables of all models are directly compared to each other and to observations in Sect. 4.1. Over the Baltic Sea catchment (Sect. 5), the model biases are much more similar so that, here, a detailed discussion for each model is not necessary. Table 3 summarizes the results of this section based on Table 4 that shows the annual mean water budget for each model as well as for the observations, and on a qualitatively judgement of the monthly means and biases. As ΔWS is zero for all models, this indicates that the hydrological cycle has been close to equilibrium over the Danube catchment at the start of the model simulations.

4.1 Intercomparison between the models

Fig. 2 shows the simulated precipitation of the models compared to CRU observations. For all models except ARPEGE the summer drying problem can clearly be seen. With ARPEGE, there is very little indication of the drying problem shown in the Danube catchment, only June and August have negative precipitation biases. REMO and CHRMs show the largest drying problem

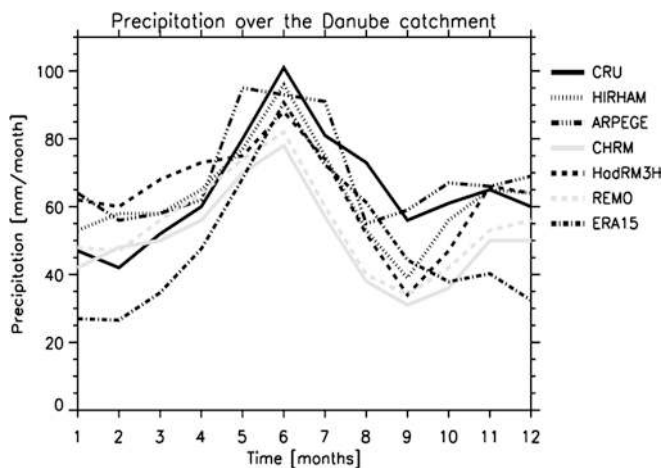


Fig. 2 Precipitation over the Danube catchment in mm/month

Table 3 Overview over regional climate model performance in the Danube catchment. ‘+’ designates overestimation, ‘-’ underestimation, ‘o’ good simulation, and ‘.’ no clear rating possible

| Simulated value | | HIRHAM | ARPEGE | CHRM | HadRM3H | REMO |
|-----------------|--------|--------|--------|------|---------|------|
| 2 m temperature | winter | o | o | - | o | o |
| | spring | o | - | - | o | o |
| | summer | + | o | o | ++ | ++ |
| | autumn | o | - | - | + | o |
| Precipitation | winter | + | + | o | + | o |
| | spring | o | o | o | o | o |
| | summer | - | o | - | - | - |
| | autumn | - | o | - | - | - |
| Evaporation | winter | + | o | o | o | o |
| | spring | . | . | . | . | . |
| | summer | + | o | - | - | - |
| | autumn | o | o | - | - | - |
| Total Runoff | winter | - | - | - | - | - |
| | spring | - | ++ | - | o | - |
| | summer | - | o | o | o | o |
| | autumn | - | o | - | - | - |
| Snowpack | winter | - | + | - | - | - |
| | spring | - | + | o | o | - |
| | Summer | o | o | o | + | o |

Table 4 Annual mean water budget in the Danube catchment. Unit: mm/month

| Hydrological variable | HIRHAM | ARPEGE | CHRM | HadRM3H | REMO | ERA | Obs. |
|-----------------------|--------|--------|------|---------|------|-----|------|
| Precipitation | 63 | 70 | 50 | 64 | 55 | 49 | 65 |
| Evapotranspiration | 55 | 47 | 39 | 45 | 43 | 50 | 44 |
| Runoff | 8 | 22 | 13 | 18 | 11 | 14 | 21 |
| DWS | 0 | 0 | 0 | 0 | 0 | - | 0 |

starting in May and lasting until December. HadRM3H and HIRHAM behave very similarly with negative precipitation biases from June to October. All models except ARPEGE are able to catch the time of the maximum precipitation in June while the latter simulates this maximum one month too early. All models except ARPEGE and REMO are also able to capture the local maximum in November. All models except CHRM and REMO overestimate precipitation in the winter. ARPEGE, HadRM3H and REMO capture the time of the minimum in February.

Fig. 3 shows the differences of the simulated 2 m temperature to CRU data. HadRM3H and REMO exhibit a large warm bias ranging from May to October. HIRHAM has a moderate warm bias in August and September while ARPEGE has a small warm bias in July and August. ARPEGE has separate cold biases in the autumn and spring while CHRM is too cold throughout the year except for the summer with maximum cold biases in March and October. In contrast to the other models that show a summer dry bias in Fig. 2 (HIRHAM, HadRM3H, REMO), CHRM does not have a summer warm bias.

Figure 4 shows the simulated evapotranspiration compared to ERA data and the quasi-observed evapotranspiration obtained from the HIRHAM run. As the latter is only a rough estimate, the results obtained from this plot have to be considered carefully. Thus, in addition a comparison of the simulated latent heat fluxes to ERA data is also included (see Fig. 5). All models tend to underestimate the evapotranspiration in the summer except for HIRHAM where evapotranspiration is lower than the observational estimate only in August and September. This underestimation is comparatively large for CHRM, HadRM3H and REMO. For HadRM3H and REMO, this may intensify their warm biases in the summer. Generally all models tend to overestimate the evapotranspiration in the winter although this seems to be significant only for HIRHAM.

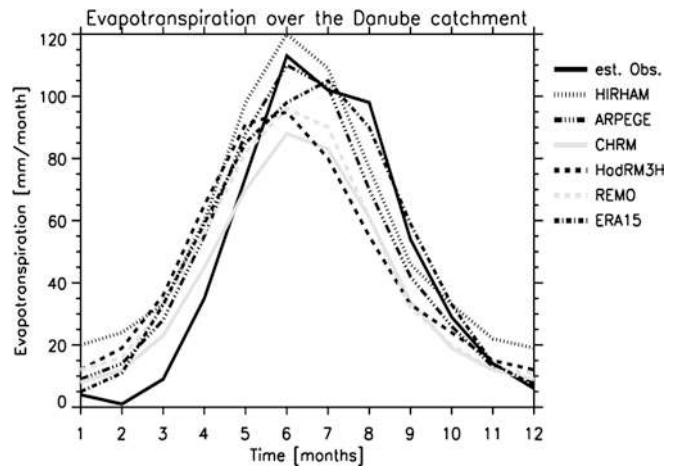


Fig. 4 Evapotranspiration over the Danube catchment in mm/month

Figure 6 shows the simulated total runoff compared to the quasi-observed runoff obtained from the HIRHAM simulation. HIRHAM and REMO largely underestimate the runoff, as CHRM does except for the peak in March. In the spring, this is related to the large underestimation of the accumulated snowpack (see Fig. 7). ARPEGE largely overestimates the snow-melt induced runoff in the spring which is related to the large overestimation of the accumulated snowpack. The latter causes also a one month delay of the runoff peak. The one month delay of the HadRM3H runoff peak is related to the fact that almost the whole model runoff is comprised of drainage from the lowest soil layer. In the HadRM3H model, the major part of the snowmelt infiltrates into the soil instead of flowing laterally as surface runoff. CHRM, REMO and HIRHAM capture the time of the runoff peak in March. All models tend to underestimate the total runoff in the winter which may be related to the overestimated evapotranspiration at the same time.

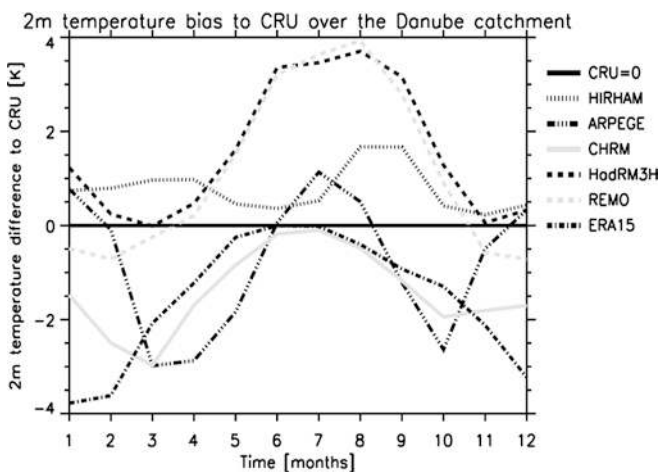


Fig. 3 The 2 m temperature difference to CRU data over the Danube catchment in K

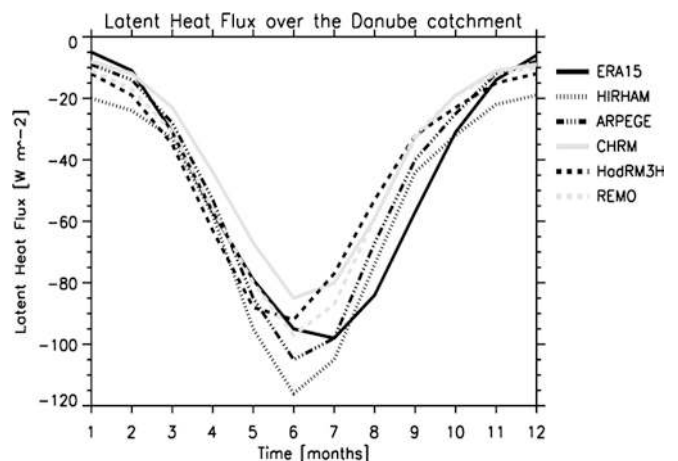


Fig. 5 Latent heat flux over the Danube catchment in Wm^{-2}

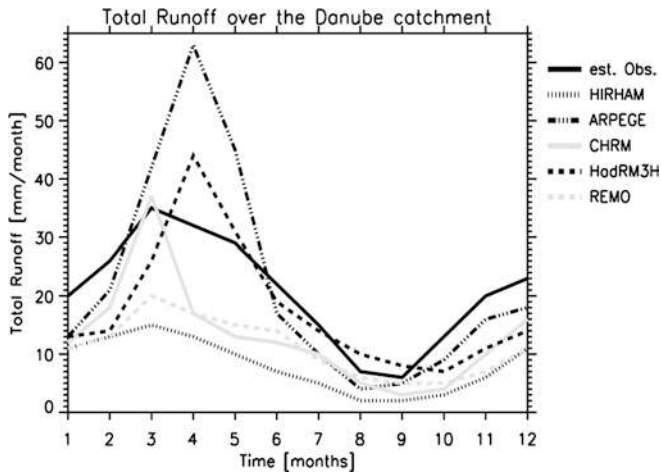


Fig. 6 Total runoff over the Danube catchment in mm/month

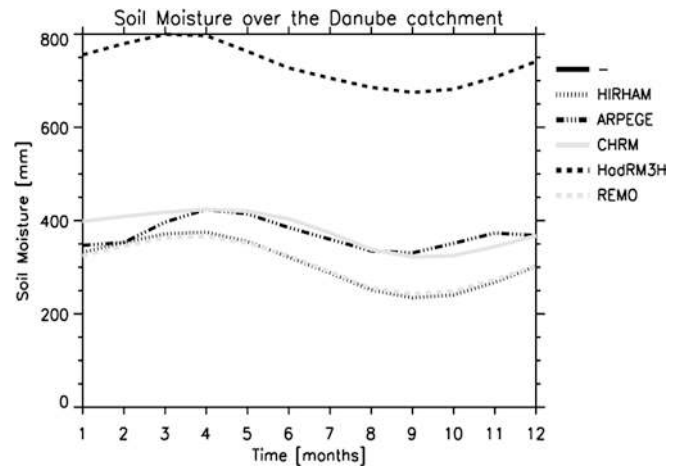


Fig. 8 Mean soil moisture in the Danube catchment in mm

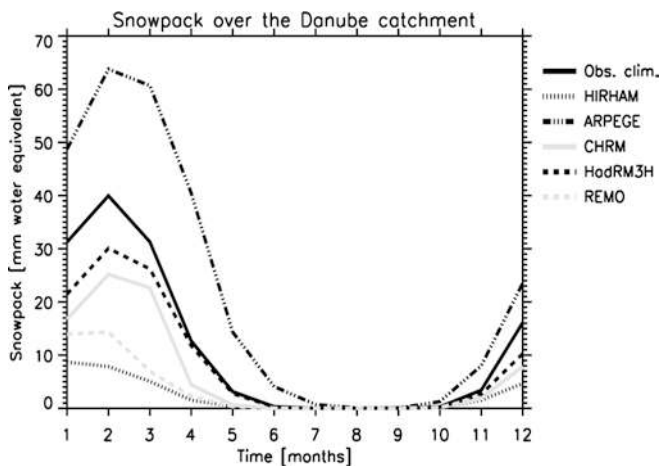


Fig. 7 Mean snowpack over the Danube catchment in mm water equivalent. USAF/ETAC climatological values of Foster and Davy (1988) are used as observed values for comparison

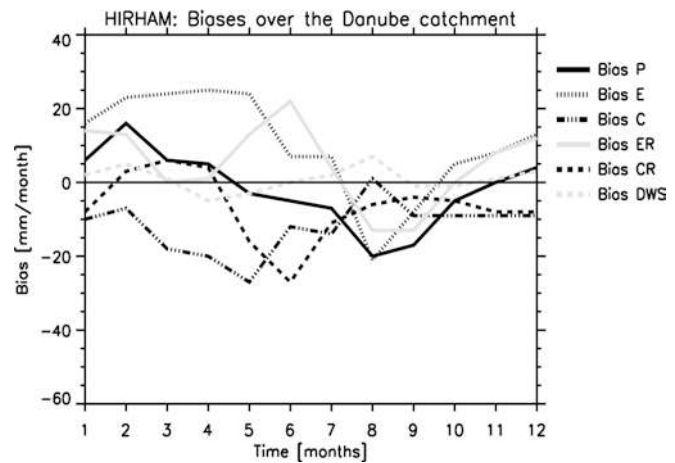


Fig. 9 Biases in the hydrological cycle of the HIRHAM simulation (1979–93) in mm/month over the Danube catchment. *P*, precipitation, *E*, evapotranspiration, *C*, convergence, *ER*, evapotranspiration (using ERA data), *CR*, convergence (using *ER*), *DWS* Storage change ΔWS

Figure 8 shows the simulated soil moisture content. As the models use different soil schemes (except for HIRHAM and REMO), one should only compare the variations in the annual cycle of the soil moisture instead of comparing its total amounts. All models except ARPEGE show similar variations and have large changes in the soil moisture during the year. ARPEGE shows a distinct April maximum which is induced by the large snowmelt.

4.2 Water and energy balances

To reach get an idea of the accuracy of the estimated evapotranspiration biases $Bias(E)$ and $Bias(ER)$ Fig. 9 is considered which shows the estimated biases of the components in the hydrological cycle (Eq. (3)) for the HIRHAM simulation (in mm liquid water per month). Comparing the $Bias(ER)$ curve with the $Bias(E)$ curve

we find a good, over all agreement, including the sign, except in the months February to May. During these months we find relatively small values of $Bias(ER)$ compared to the relatively large values of $Bias(E)$. This constitutes a significant difference between the two estimates in the months February to May.

Hagemann et al. (2002) have shown that for the estimate of $Bias(E)$ too small values of the quasi observed E_{obs} determined from Eq. (1) were used, because the ΔWS_{obs} (see Appendix 1), and to a much lesser extent also the R_{obs} , are estimates are too large. We have used the HIRHAM simulation to determine both sets of coefficients so that errors in their values may be caused by inaccuracies in the HIRHAM model. The main reason seems to be the systematic error in the HIRHAM snowpack, see Fig. 7, namely the unrealistically low snow pack simulated during the winter and thus an unrealistic small snow melt during the spring. On the

other hand, in ERA almost the whole snowmelt infiltrates into the soil (Hagemann and Dümenil Gates 2001) so that the soil is much wetter than in reality which may cause an overestimation of evapotranspiration in the melting period which would yield in an underestimation of $Bias(ER)$. This would be consistent with the overestimation of the annual evapotranspiration shown in Table 2. Taking the errors in the spring of both evapotranspiration estimates into account, we assume that the $Bias(ER)$ and the corresponding $Bias(CR)$ estimates may be more realistic in the winter and spring than the $Bias(E)$ and $Bias(C)$ estimates, respectively. Alternatively, true convergence can be estimated directly from ERA and so a convergence bias calculated by comparing this with convergence calculated in the models. This has been done in the case of the HadRM3H model.

4.2.1 HIRHAM

Figure 10, which shows the deviations of the HIRHAM surface energy fluxes from ERA, indicates that the solar radiation at the surface in the HIRHAM simulation is estimated to be excessive throughout the year. Considering the fact that the ECHAM4 short wave radiation scheme, which is used in HIRHAM, has been validated to behave realistically (Wild et al. 1996), it seems most likely that the reason for the excessive solar radiation is a too small cloud cover. The excessive solar radiation leads to too high surface air temperatures (Fig. 3) and probably a too unstable boundary layer, which both lead to excessive evapotranspiration (Fig. 9) as long as sufficient soil moisture is available. The too high temperatures in winter may, at least partly, explain also the too small snow pack (Fig. 7) simulated. During spring small temperature biases over areas of snow melt seem to explain the estimated small evapotranspiration biases in that season. Due to compensating for excessive

divergence of moisture, apparently caused by systematic errors in the general a-geostrophic circulation of the atmosphere, the excessive evapotranspiration is not returned to the soil in the catchment in the form of a similar amount of excessive precipitation. On the contrary, the divergence of moisture seems to dominate during the months May to July which leads to negative precipitation biases in the summer and autumn seasons (Fig. 9). This and the excessive evapotranspiration contribute to an excessive drying of the model soil (reaching its minimum in September, see Fig. 8), which is becoming so dry that the evapotranspiration bias turns negative in August and September, in spite of too high surface air temperatures. The long term balance of soil moisture is maintained by a negative bias in runoff throughout the year. Thus, in the model the catchment as a whole loses an excessive amount of moisture through its lateral boundaries in the atmosphere, but saves a similar amount of moisture by too little integrated runoff, or in other words by too little discharge from the catchment.

Earlier results, Wild et al. (1995) making a one-column simulation with the HIRHAM surface scheme driven with observed atmospheric data from the Cabauw site and Hagemann et al. (2001) making 3D HIRHAM model experiments testing the sensitivity to changes in prescribed initial (1st July) soil moisture, have indicated that deficiencies in the model representation of the land surface processes cannot be a main reason for the summer drying problem of HIRHAM. Thus, we conclude that, as the reason for the too large solar radiation at the surface seems to be systematic, too little cloud cover is probably caused by an error in the parametrization which should be investigated. Further, it should be investigated if wether there are other reasons than those suggested here for the periods of excessive evapotranspiration. Also the reason(s) for too little snow pack other than the excessive emperature should be located. The fact that the HadRM3H model simulation has almost the right snow pack, in spite of winter temperatures approximately similar to those in the HIRHAM simulation, indicates that the insufficient snow pack is not caused by too smooth mountains in HIRHAM as has been suggested previously for Scandinavia (Christensen et al. 1998).

This whole analysis is described in more detail in Hagemann et al. (2002).

4.2.2 ARPEGE

ARPEGE simulates too much convergence in the winter (see Fig. 11) which is consistent with the overestimated precipitation and the accumulated snowpack. In the spring, too little convergence is simulated. It seems that the convergence of moisture into the catchment is weakened due to too much moisture in the atmosphere which may partly be caused by the overestimated evapotranspiration. As there is also less upward surface solar radiation than in the ERA data (see Fig. 12), this

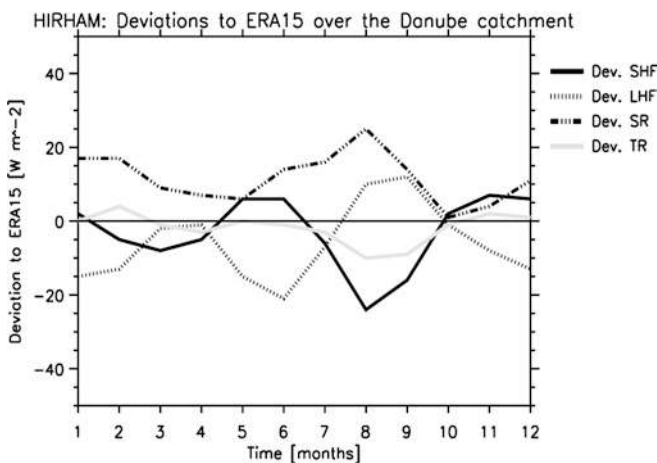


Fig. 10 Deviations from ERA of the surface energy fluxes of the HIRHAM simulation (1979–93) in Wm^{-2} over the Danube catchment SHF , sensible heat flux, LHF , latent heat flux, SR , surface solar radiation, TR , surface thermal radiation

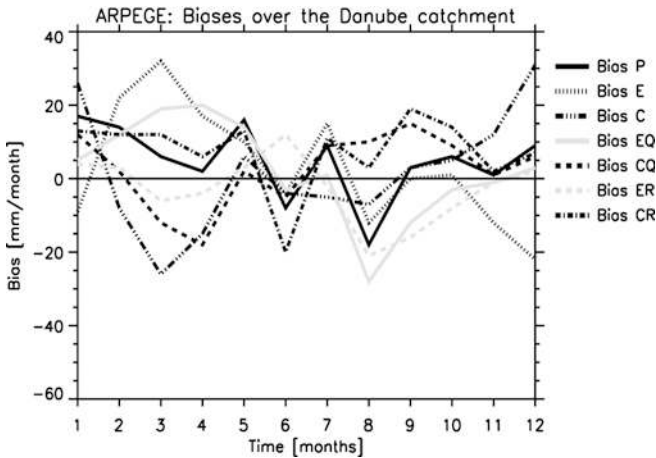


Fig. 11 Biases in the hydrological cycle of the ARPEGE simulation (1979–93) in mm/month over the Danube catchment. *P*, precipitation, *E*, evapotranspiration, *C*, convergence, *EQ*, evapotranspiration (2nd estimate), *CQ*, convergence (using *EQ*), *ER*, evapotranspiration (using *ERA* data), *CR*, convergence (using *ER*)

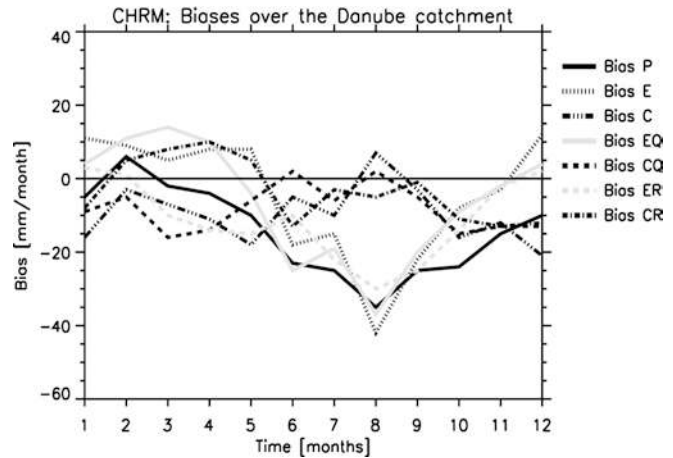


Fig. 13 Biases in the hydrological cycle of the *CHRM* simulation (1979–93) in mm/month over the Danube catchment. *P*, precipitation, *E*, evapotranspiration, *C*, convergence, *EQ*, evapotranspiration (2nd estimate), *CQ*, convergence (2nd estimate), *ER*, evapotranspiration (using *ERA*, data), *CR*, convergence (using *ER*)

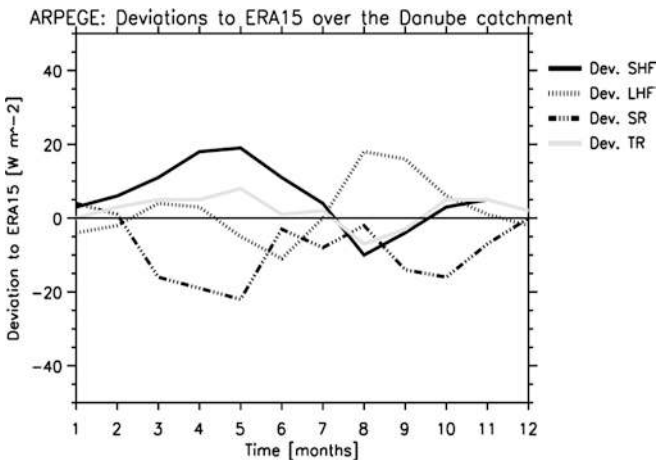


Fig. 12 Deviations from *ERA* the surface energy fluxes of the ARPEGE simulation (1979–93) in Wm^{-2} over the Danube catchment *SHF*, sensible heat flux, *LHF*, latent heat flux, *SR*, surface solar radiation, *TR*, surface thermal radiation

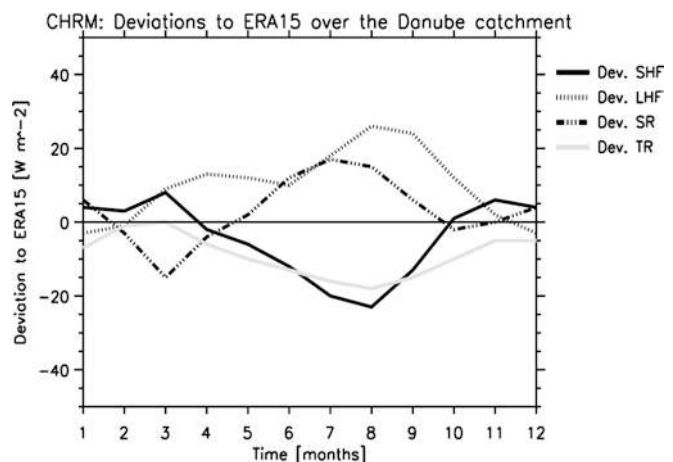


Fig. 14 Deviations from *ERA* of the surface energy fluxes of the *CHRM* simulation (1979–93) in Wm^{-2} over the Danube catchment *SHF*, sensible heat flux, *LHF*, latent heat flux, *SR*, surface solar radiation, *TR*, surface thermal radiation

may indicate too much simulated cloud cover in the spring. In principle, too little upward surface solar radiation may also be caused by a too low albedo. However the largely overestimated snow cover would suggest imply a too large albedo. Moreover the overestimated snow cover seems to cause an underestimation of the upward (negative) sensible heat flux at the same time.

4.2.3 *CHRM*

During the summer the large negative bias in precipitation (Fig. 13) is almost compensated by the bias in evapotranspiration so that the bias in convergence is small. This indicates that the summer drying problem is

not related to the atmospheric transport of moisture into the area. The too little upward latent heat flux compared to *ERA* (see Fig. 14) corresponds well with the underestimated evapotranspiration in the summer. Since the 2 m temperatures are too cold throughout the year except during the summer (see Fig. 3) it was initially thought that this may be related to a too large albedo (see below). In the summer, the effect that causes the too cold temperatures seems to be compensated by too little cloud cover as indicated by too large surface solar radiation accompanied by over large upwards sensible heat flux and surface thermal radiation. The underestimation of cloud cover is presumably induced by the underestimated evapotranspiration that provides the atmosphere with insufficient moisture.

The surface albedo (not shown), when compared to ERA fields, shows very good agreement for snow-free values, while retaining a good yearly cycle connected to the snow cover. Experiments with the relationship between the snow amount, the snow cover and the total surface albedo have resulted in very small sensitivities. Since the snow amount, snow melt and runoff all seem quite correct, surface albedo does not seem to hold the explanation for the surface radiative balance problem.

During the early spring, a lessening of the surface solar deficit is shown (Fig. 14), which has been however partitioned into producing a slightly larger summer (about 15 W/m^2) peak of positive solar bias which seems to cause a slightly larger sensible heat bias and corresponding slightly more negative latent heat (more than 20 W/m^2) and positive thermal radiation biases. Therefore it is plausible that errors in the soil-vegetation-atmosphere transfer scheme (SVATS) could be the cause for the local tendency of the model to become dry and warm over summer, since the energy lost in sensible heat and thermal radiation should and could be used for evapotranspiration. The biases in precipitation and their explanation (see earlier) agree with this.

In the winter the error in the 2 m temperature (see Fig. 3) seems to track the signal in the ERA-15 data but is certainly smaller (-3 to -2 K versus -4 K). This may indicate a connection with a signal from the driving data travelling through the model domain from the lateral boundaries. However this explanation should be more valid for grid points near the domain boundaries. A simulation for one season with altered near-surface lateral boundary conditions does not show a large impact on the simulated temperatures.

An analysis of the daily minimum and maximum 2 m temperatures over Europe has shown that the minimum temperatures are simulated too high and the maximum temperatures are simulated too low, especially in the south. This is induced by the force restore soil model which uses a 1-year time scale bottom boundary condition that constrains the surface temperature oscillation. Therefore the diurnal cycle is dampened, and it might be that the diurnal cycle is also shifted in time as the time constant of 1 year introduces a phase error in the top (thin) layer of soil which should represent the diurnal oscillation. Jacobsen and Heise (1982) have shown that the phase error can be as large as 50% on the limb of the two periods represented by the time constants in the model (1day, 1 year) and that the time shift can be of several hours. This will be further examined in studies that are planned with a multi-layer soil model.

4.2.4 HadRM3H

Considering the quasi-observed evapotranspiration obtained from the HadRM3H simulation, the dry bias in precipitation (Fig. 15) is almost compensated by the bias in evapotranspiration which yields no significant bias in convergence. But if EQ_{obs} obtained from the HIRHAM simulation is considered, a positive convergence bias in

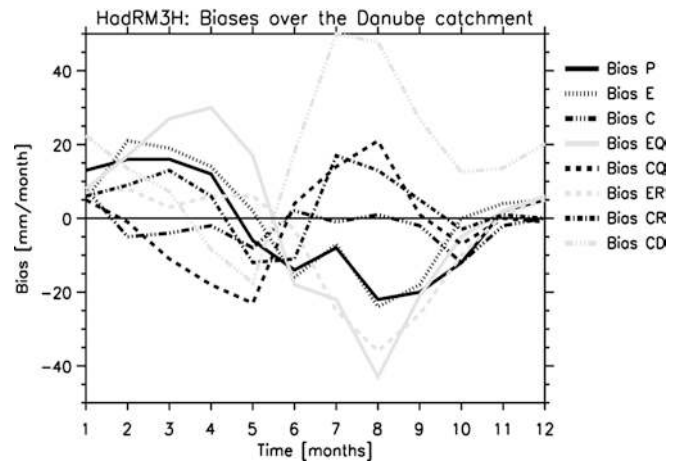


Fig. 15 Biases in the hydrological cycle of the HadRM3H simulation (1979–92) in mm/month over the Danube catchment. *P*, precipitation, *E*, evapotranspiration, *C*, convergence, *EQ*, evapotranspiration (2nd estimate), *CQ*, convergence (2nd estimate), *ER*, evapotranspiration (using ERA data), *CR*, convergence (using ER) *CD*, convergence (using direct estimate)

the summer and a negative convergence bias in the spring can be seen. The underestimation of the upward latent heat flux compared to ERA (Fig. 16) corresponds to values that lie in between the two evapotranspiration biases. This demonstrates the large uncertainty in the estimate of the observed evapotranspiration. At the same time, the upward sensible heat flux and the upward surface thermal radiation are much larger than ERA data as well as the downward surface solar radiation which is larger throughout the year. Thus, there is too much absorption of energy in the soil which causes the severe warm bias (Fig. 3) and which is a clear indicator for a too low albedo. The low albedo is directly connected to a lack of clouds which itself is induced by the fact that not enough moisture is advected into the region

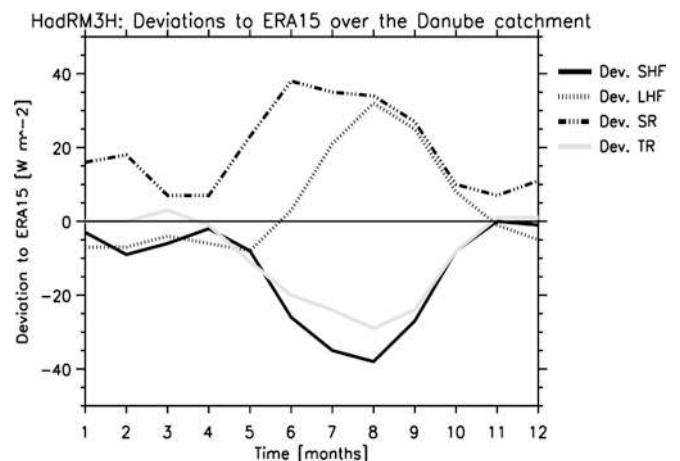


Fig. 16 Deviations from ERA of the surface energy fluxes of the HadRM3H simulation (1979–92) in W m^{-2} over the Danube catchments *SHF*, sensible heat flux, *LHF* latent heat flux, *SR* surface solar radiation, *TR* surface thermal radiation

as indicated by the negative convergence bias CQ_{obs} in the spring (Fig. 15).

These factor implies that the overestimation of precipitation seen in the first two months of spring results from too high evaporation and, as the evaporation bias is larger than the precipitation bias, the convergence bias (from the definition in Eq. 3) is negative. The precipitation bias then changes sign in May whilst the evaporation bias is still positive and thus the convergence bias becomes even more negative. This implies that there is a strong circulation component in the cause of the dry bias in May and suggests that this is the underlying cause of the subsequent warm and dry bias throughout summer. This is supported by an anomaly (HadRM3H compared to ERA) in the 500 hPa geopotential height of over 30 m over major parts of Central and Southern Europe with a maximum of over 50 m centred over the Balkans. This anomaly is probably a non-physical response of the RCM to initial warming over this region which acts to intensify the summer drying problem by enhancing the blocking potential. The lack of convergence restricts precipitation and associated clouds which thus (further) increases the short wave radiation and surface heating/temperature. The evaporation is then able to balance most of this heating in May but this depletes soil moisture sufficiently to limit this mechanism, and also evaporation to maintain the hydrological cycle, throughout summer.

In order to investigate further the large discrepancies in convergence biases in summer, direct calculations of convergence were made from the ERA data and the RCM. These supported the negative convergence biases in April and May as well as the positive biases in the summer months seen in the CQ and CR estimates. In fact, this direct ERA-derived estimate of the convergence biases was even more positive in summer than these other two estimates suggested (CD in Fig. 15). This is consistent with the idea that the other convergence bias estimates may be underestimated as a result of low estimates of the change in water storage (see Sect. 3). This effect will clearly be most severe when the convergence bias is estimated from the HadRM3H results as this model has a large warming resulting from severe limitations on the evapotranspiration (and thus small changes in soil moisture). This is confirmed as in this case the convergence bias is close to zero supporting the theory that using the HadRM3H water storage/precipitation relationship leads to low estimates of observed, and so insufficiently negative (in this case) biases in, evapotranspiration.

4.2.5 REMO

REMO shows large negative biases in precipitation and evapotranspiration ranging from the late spring to the autumn (Fig. 17). The large underestimation of the summer evapotranspiration is directly related to the overestimation of the 2 m temperature (see Fig. 3). The first intensifies the dry bias in precipitation and the latter

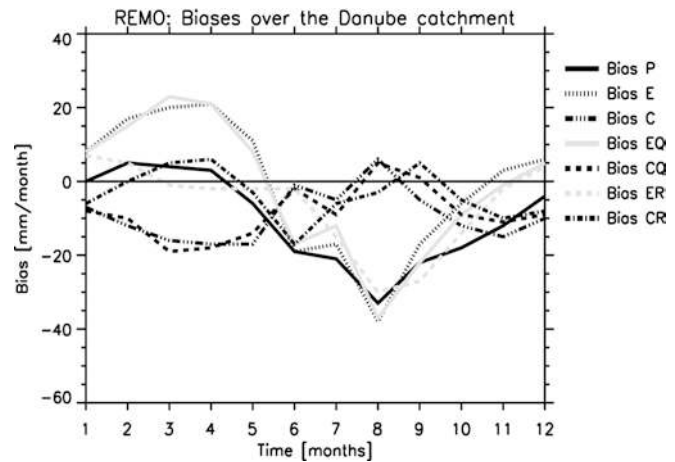


Fig. 17 Biases in the hydrological cycle of the REMO simulation (1979–93) in mm/month over the Danube catchment. P , precipitation, E , evapotranspiration, C , convergence, EQ , evapotranspiration (2nd estimate), CQ , convergence (2nd estimate), ER , evapotranspiration (using ERA data), CR , convergence (using ER)

causes the too large negative upward flux of surface thermal radiation (Fig. 18). The warm temperature bias is caused by insufficient convective activity, which leads to a too small amount of clouds and precipitation in the summer, thereby allowing a too strong radiative heating of the surface indicated by too large downward surface solar radiation and too large upward sensible heat flux compared to ERA data in the summer.

As REMO has somewhat less evapotranspiration than HIRHAM in the spring, the soil is slightly moister and, in principle, about the same amount or even more water is available for evapotranspiration in the summer. But the fact that the REMO summer evapotranspiration is much less than in HIRHAM may suggest that the advection of dry air and so the divergence of moisture out of the Danube catchment is

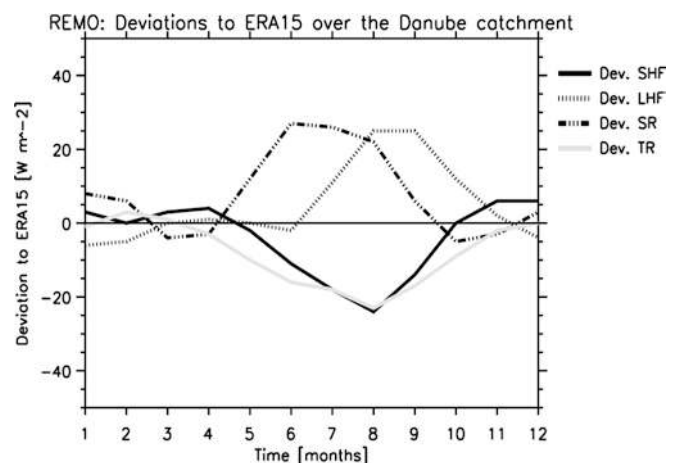


Fig. 18 Deviations from ERA of the surface energy fluxes of the REMO simulation (1979–93) in Wm^{-2} over the Danube catchment. SHF , sensible heat flux, LHF , latent heat flux, SR , surface solar radiation, TR , surface thermal radiation

considerably smaller than in HIRHAM. Similar behaviour is seen in CHRM which shares the same dynamics as REMO indicating that this is a feature of the model dynamics rather than being driven by the physics which REMO shares with HIRHAM. A detailed investigation of the mean atmospheric circulation is under preparation.

5 The Baltic Sea catchment

The location of the Baltic Sea catchment is shown in Fig. 1. Its area comprises about 17,29,000 km² and the annual mean discharge into the Baltic Sea is about 15,323 m³/s (483 km³/a). As in Sect. 4, all atmospheric variables were integrated over the whole catchment area and the water fluxes will be expressed in mm/month instead of a volume flux unit. In Sect. 5.1, the different simulated variables of all models are directly compared to each other and to observations, and the biases in the water balances and the deviations from ERA data in the energy balance are analysed. Table 5 summarizes the results of this section based on Table 6 that shows the annual mean water budget for each model as well as for the observations, and on a qualitative judgement of the monthly means and biases. Again, $\Delta WS = 0$ for all models indicates that the hydrological cycle was close to equilibrium over the Baltic Sea catchment at the start of the model simulations.

5.1 Intercomparison between the models

Figure 19 shows the difference of the simulated 2 m temperature to CRU data for each model. The only common feature seems to be the tendency temperatures in the spring to be too low. Otherwise the models behave differently. For HIRHAM and HadRM3H, the difference of the simulated 2 m temperature and CRU data is small throughout the year. The CHRM 2 m temperature

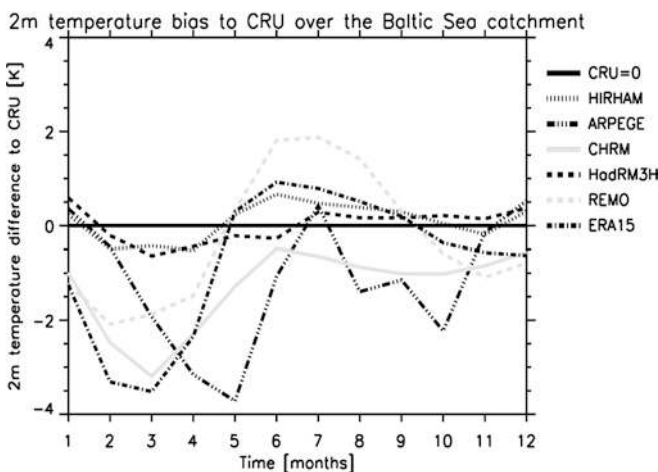


Fig. 19 The 2 m temperature difference to CRU data over the Baltic Sea catchment in K

Table 5 Overview over regional climate model performance in the Baltic Sea catchment. ‘+’ designates overestimation, ‘-’ underestimation, ‘o’ good simulation, and ‘.’ no clear rating possible

| Simulated value | | HIRHAM | ARPEGE | CHRM | HadRM3H | REMO |
|-----------------|--------|--------|--------|------|---------|------|
| 2 m temperature | winter | o | o | - | o | - |
| | spring | o | - | - | o | - |
| | summer | o | o | o | o | + |
| | autumn | o | - | - | o | o |
| Precipitation | winter | + | + | + | + | + |
| | spring | + | + | + | + | + |
| | summer | o | o | + | o | o |
| | autumn | + | + | o | + | + |
| Evaporation | winter | + | o | o | o | o |
| | spring | + | . | . | . | . |
| | summer | . | . | . | . | . |
| | autumn | . | . | . | . | . |
| Total Runoff | winter | - | - | o | o | o |
| | spring | - | ++ | o | - | o |
| | summer | - | o | o | + | o |
| | autumn | - | o | o | o | o |
| Snowpack | winter | - | + | o | o | o |
| | spring | - | + | o | o | o |
| | Summer | o | o | o | + | o |

Table 6 Annual mean water budget in the Baltic Sea catchment. Unit: mm/month

| Hydrological variable | HIRHAM | ARPEGE | CHRM | HadRM3H | REMO | ERA | Obs. |
|-----------------------|--------|--------|------|---------|------|-----|------|
| Precipitation | 58 | 62 | 60 | 62 | 62 | 48 | 51 |
| Evapotranspiration | 45 | 32 | 37 | 37 | 39 | 41 | 28 |
| Runoff | 12 | 29 | 21 | 21 | 20 | 17 | 23 |
| DWS | 0 | 0 | 0 | 0 | 0 | - | 0 |

is generally too cold with a maximum bias in the spring, and it seems that the CHRM temperature bias tracks the ERA data very closely in the winter and early spring. ARPEGE has cold biases in the spring and the autumn which are similar to the ARPEGE biases over the Danube catchment (see Sect. 4.1). REMO seems to have an over-enhanced annual cycle in the 2 m temperature as it has a cold bias in the winter and early spring, and a warm bias in the summer.

For all models, the comparison of simulated precipitation to CRU observations (Fig. 20, and Fig. 21 for the bias) shows the common atmospheric model feature of the overestimation of precipitation over the Baltic sea catchment from the autumn to the spring. This may in part be related to systematic errors in the mean sea level pressure fields that correspond to errors in the near surface general circulation (Machenhauer et al. 1996, 1998) but given that quasi-observed boundary conditions are being used implies a positive bias due to errors in the model physics. In the summer, all models simulate realistic precipitation amounts although they simulate the precipitation maximum in July instead of August. All models except ARPEGE capture the time of the minimum precipitation in February. It should be mentioned that precipitation measurements in high latitudes tend to underestimate the snowfall amounts. Thus, precipitation data (1981-93) from the BALTEX database (BHDC, SMHI 2001) are also given in Fig. 20 which are in a very good agreement with the CRU precipitation. Further investigations by Rubel and Hantel (2001) for the period 1996-1998 indicate that the uncorrected BALTEX precipitation data should be corrected by about 13% annually. The necessary correction is largest in February and smallest in August. If a similar correction for the ERA15 period is applied, the annual observed precipitation would equal about 58 mm/month, and consequently the observed evapotranspiration would equal about 35 mm/month.

Figure 21 shows the biases in the hydrological cycle for all RCMs. Keeping the uncertainties in the estimates

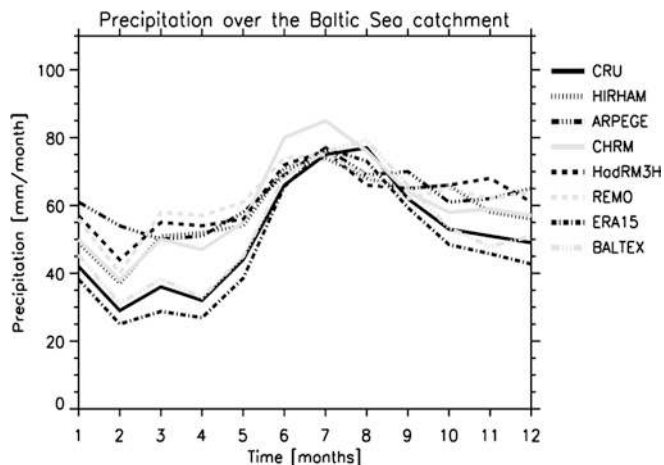


Fig. 20 Precipitation over the Baltic Sea catchment in mm/month

of observed evapotranspiration in mind (see also Sect. 3), it can be stated that all models overestimate the evapotranspiration in spring while they seem to have reasonable amounts in summer. The overestimation of evapotranspiration in the spring seems to moisten the atmosphere too much so that there is too little convergence of moisture from other regions. Further characteristics of the model simulations related to the biases of the hydrological cycle and the deviations of the surface energy fluxes from ERA data shown in Fig. 22 are discussed briefly for each model separately.

For HIRHAM, the overestimated evapotranspiration is consistent with the variation of the simulated latent heat flux (negative upward) from the ERA data (Fig. 22a). The upward surface thermal radiation is larger than ERA data in winter and spring which seems to be related to the underestimated snow cover (Fig. 24). The latter probably also causes a too low albedo as indicated by an overestimated surface solar radiation in the winter. Since this is compensated by an overestimation in the latent heat flux, the 2 m temperatures are simulated well (Fig. 19). The insufficiency surface solar radiation in the summer is partially compensated by too little upward sensible heat flux at the same time.

For ARPEGE, the deviations of the surface energy fluxes from ERA data (Fig. 22b) reveal that the downward surface solar radiation is far too low from April to September which seems to be related to a too large background albedo. This is supported by the fact that this deviation is close to zero when snow is covering the surface during the winter (Fig. 24). An underestimated cloud cover does not seem to be responsible for this deviation since precipitation is simulated quite well at the same time. The underestimated heating by the too low surface solar radiation also causes the cold biases in the spring and the fall (Fig. 19). Only in July does this seem to be compensated by other effects.

For CHRM, the positive precipitation bias (Fig. 21c) is almost compensated by the positive evapotranspiration bias except in the spring when the latter is much larger. At the same time, CHRM simulates too little surface solar radiation compared to ERA (Fig. 22c). This underestimation may be related to too much cloud cover which is supported by the large spring cold bias of the 2 m temperature (Fig. 19) and the corresponding too small upward sensible heat flux. Originally it was thought that the underestimation of surface solar radiation may be related to a too large albedo but the snow-free albedo values over land (not shown) correspond well to the ones in the ERA data set. Despite the too cold temperatures the snow cover and the snowmelt (see Fig. 24) are simulated quite well which suggests that the surface albedo is also not responsible for the biases in the spring. As the latent heat flux is comparatively close to the ERA data, the SVATS seems to perform well in this region.

In an earlier version of the CHRM model (Vidale et al. 2003), a large negative bias in surface solar radiation (up to -50 W/m^2 in May/June) was present. This

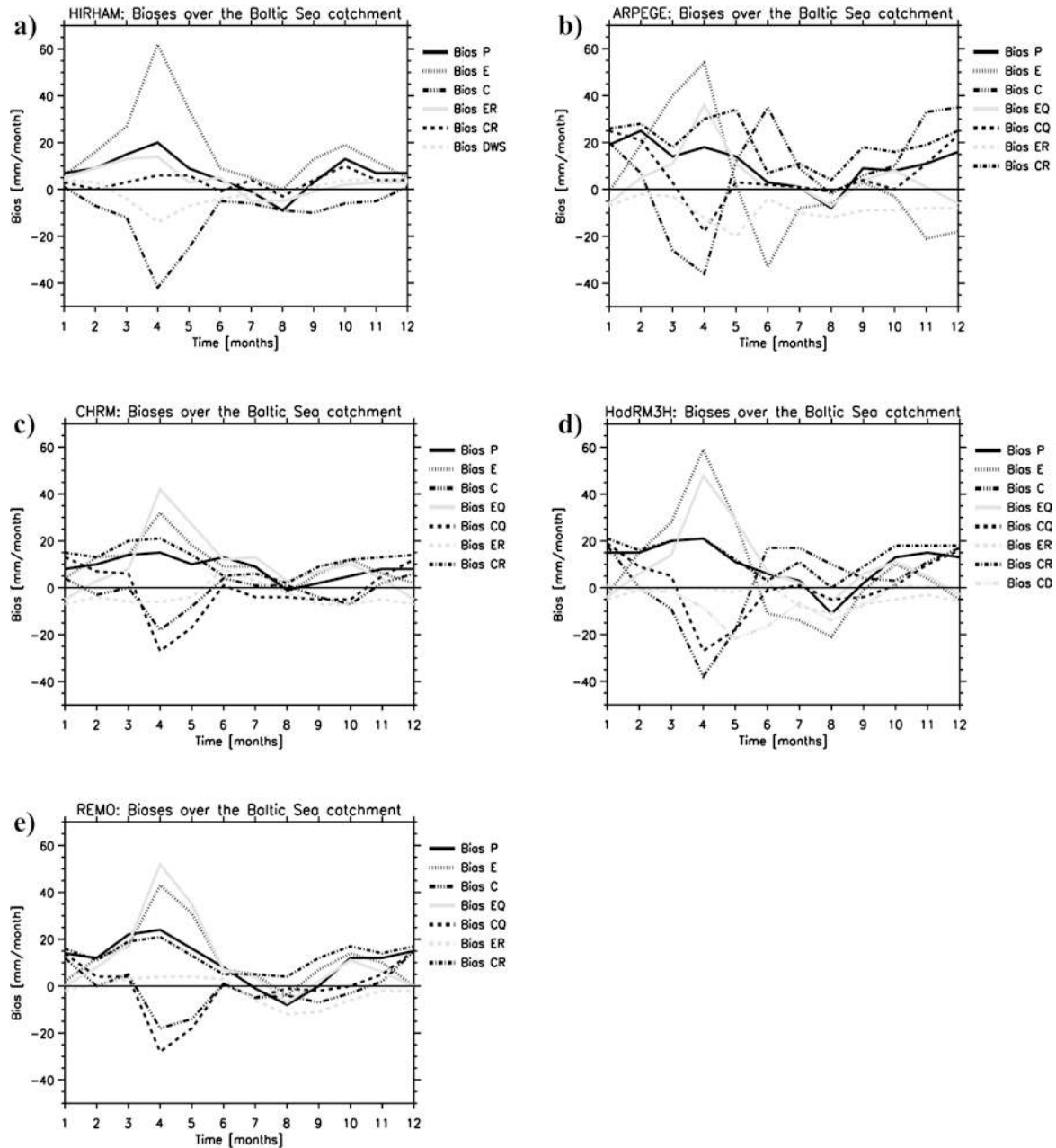


Fig. 21 Biases in the hydrological cycle in mm/month over the Baltic Sea catchment for **a** HIRHAM simulation (1979–93), **b** ARPEGE simulation (1979–93), **c** CHRM simulation (1979–93), **d** HadRM3H simulation (1979–92), **e** REMO simulation (1979–93), *P*, precipitation, *E*, evapotranspiration, *C*, convergence, *EQ*,

evapotranspiration (2nd estimate), *CQ*, convergence (2nd estimate), *ER*, evapotranspiration (using ERA data), *CR*, convergence (using ERA), *CD*, convergence (using direct estimate in **d**, in **a**: *DWS* Storage change ΔWS)

bias has been clearly reduced (extreme of $-20 W/m^2$ in May) by the restoration of surface solar radiation, which had been strongly depressed by the low level clouds diagnosed by the Slingo (1987) cloud scheme with the enhanced summer moisture flux. This was accomplished by implementing the Xu and Randall (1996) cloud diagnostics, which mainly affect the liquid water path seen by the radiation rather than the distribution of cloud types which were not substantially modified. Concurrently, the biases in other components of the

surface energy balance were also reduced, in particular the negative sensible heat bias in the summer.

For HadRM3H, the overestimated evapotranspiration in spring seems to be caused by inadequate handling of the snowmelt which almost completely infiltrates into the soil (see Sect. 4.1). Thereby, the large negative spring runoff bias (Fig. 23) is caused and the soil becomes too wet which results in the overestimated evapotranspiration. Figure 22d does not show an overestimation of latent heat flux compared to ERA. This can be explained

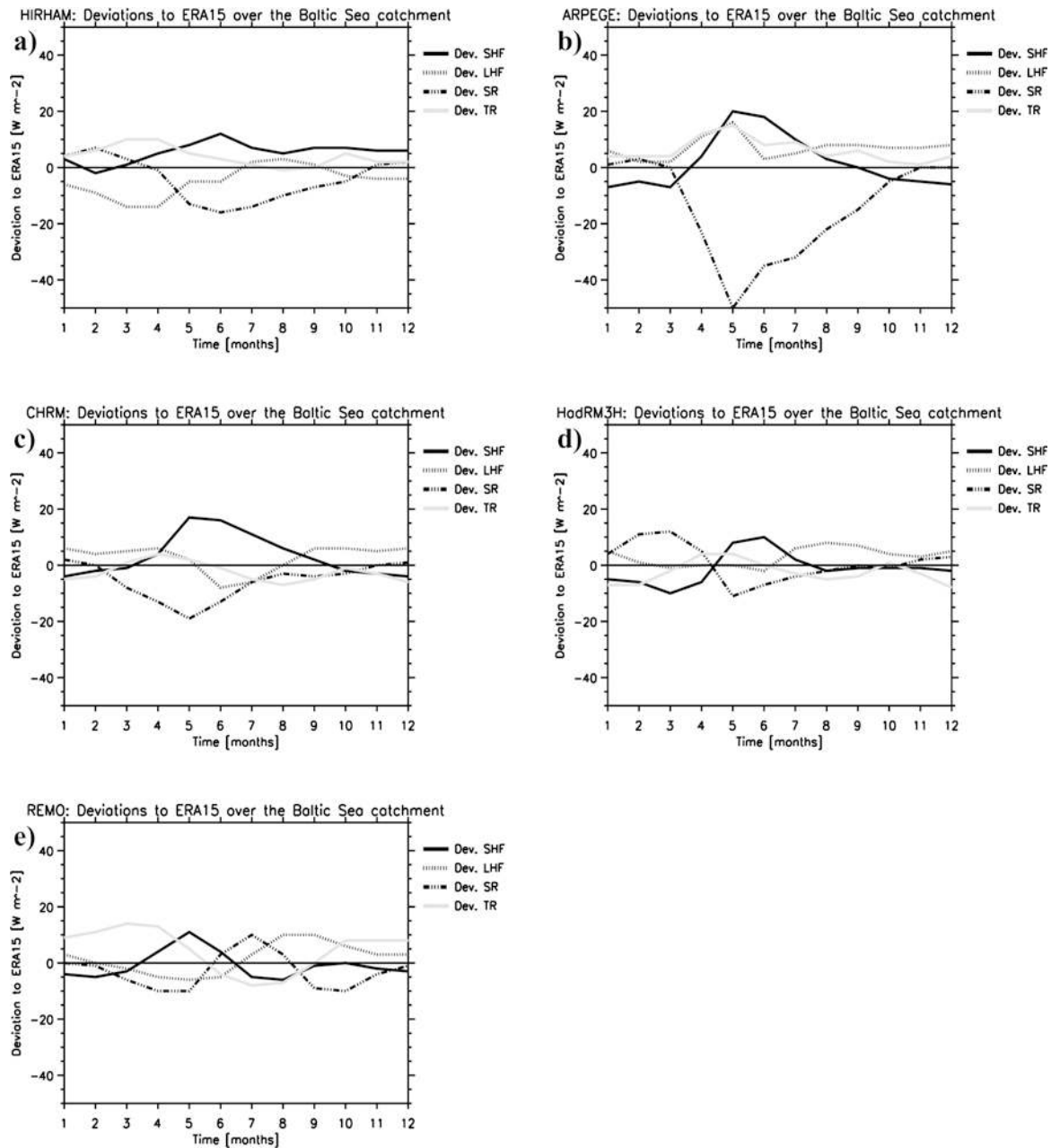


Fig. 22 Deviations of the surface energy fluxes from ERA in Wm^{-2} over the Baltic Sea catchment for **a** HIRHAM simulation (1979–93), **b** ARPEGE simulation (1979–93), **c** CHRM simulation (1979–93), **d** HadRM3H simulation (1979–92), **e** REMO simulation

by the fact that the ERA surface scheme behaves very similarly in the unrealistic treatment of the snowmelt (see Hagemann and Dümenil Gates 2001). Thus, the latent heat flux and the evaporation of ERA are highly unreliable in regions and months where the snow is melting. Since the 2 m temperature in spring is simulated well (Fig. 19), the snow albedo may be too low. This is supported by too much downward surface solar radiation and too much upward surface thermal radiation during the winter (Fig. 22d).

For REMO, the deviation of the upward surface thermal radiation to ERA data (Fig. 22e) closely follows the 2 m temperature bias (Fig. 19), with too large values

in the summer and too low values in the winter and early spring. The temperature bias may be caused by deficits in the simulation of clouds, as the too large downward surface solar radiation in the summer may be related to an underestimation of cloud cover and the too little surface solar radiation in the spring and autumn may be related to an overestimation of cloud cover. Another reason contributing to the temperature bias may be the absence of a seasonal cycle in the vegetation in REMO. HIRHAM, where a seasonal variation of LAI and vegetation ratio is implemented, shows almost no temperature bias in the Baltic Sea catchment (Fig. 19). An implementation of a seasonal vegetation cycle into

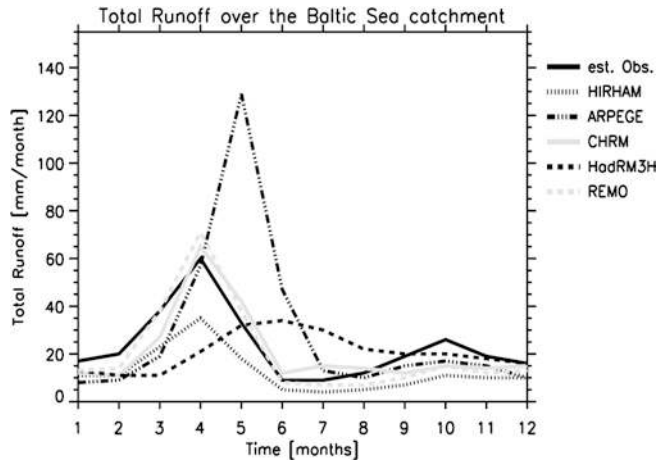


Fig. 23 Total runoff over the Baltic Sea catchment in mm/month

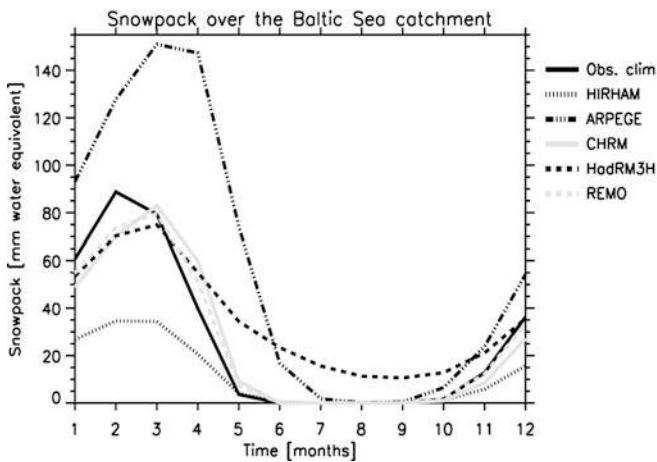


Fig. 24 Mean snowpack over the Baltic Sea catchment in mm water equivalent. USAF/ETAC climatological values of Foster and Davy (1988) are used as observed values for comparison

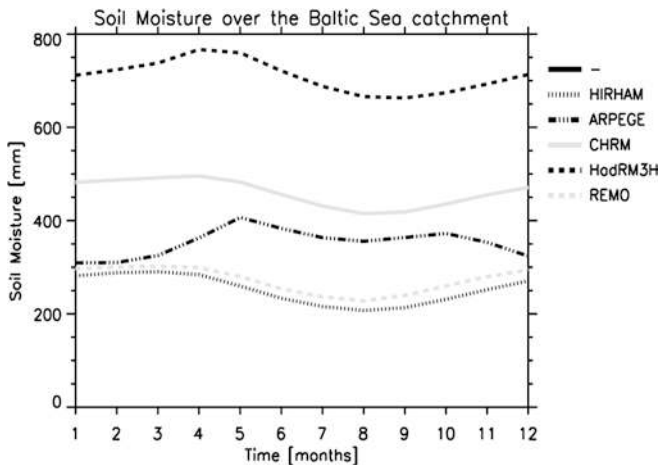


Fig. 25 Mean soil moisture in the Baltic Sea catchment in mm

REMO (Vs. 5.1) has lead to an increase in summer evapotranspiration (cooling of the surface) and a decrease in winter evapotranspiration (less cooling of the surface) so that the temperature bias is reduced.

Figure 23 shows the simulated total runoff compared to the quasi-observed runoff obtained from the HIRHAM simulation. The results of this comparison are quite similar to the results obtained for the Danube catchment (see Sect. 4). This indicates that HIRHAM has a general tendency to underestimate runoff as well as the accumulated snowpack (Fig. 24), while ARPEGE largely overestimates the accumulated snowpack which results in an overestimated snowmelt induced runoff peak in spring and in a delay of this peak. This delay is also connected to the too cold 2 m temperatures in spring (see Fig. 19). For HadRM3H, the fact that there is almost no surface runoff generally smoothes the total runoff curve and, thus, the soil is filled by the snowmelt (Fig. 25) and the runoff peak seems to be caused by rain falling on the full soil moisture reservoirs. REMO and CHRM simulate the runoff very well even though they underestimate the runoff during the autumn. Again, CHRM, REMO and HIRHAM capture the time of the runoff peak in April and all models tend to underestimate the total runoff in the winter which may be related to the overestimated evapotranspiration at the same time. The good simulation of the spring runoff peak of CHRM and REMO is consistent with their simulation of the accumulated snowpack (Fig. 24) during spring. HadRM3H shows the strange characteristic that it has snow throughout the year within the catchment. These amounts of snow are simulated in several grid boxes in the mountains of Norway where the summer snowpack reaches up to 5 m in one gridbox, which is unrealistic. This is caused by too cold model temperatures at those high elevations so that the snow does not melt in summer.

All models except for ARPEGE show an increase in soil moisture (Fig. 25) from autumn to the winter. The ARPEGE soil moisture decreases although its precipitation increases at the same time. This indicates that the precipitation falls as snow instead of rain (as it should) which corresponds to the overestimation of the snowpack. As mentioned before, the HadRM3H snowmelt fills the soil in the spring thereby increasing the soil moisture much more than the other models (except for ARPEGE).

6 Conclusions

In this study, the water and energy budgets simulated by five regional climate models applied over Europe were compared. Work focused on two large catchments with different climates. For the Baltic Sea catchment that represents a maritime climate, all models show a similar simulation of precipitation which is overestimated throughout the year except during the summer, and which represents the annual cycle of precipitation quite well.

As the advection of moisture does not seem to be a major error source for this overestimated precipitation, it is probably caused by the internal model parametrizations, such as the large-scale condensation and the convection schemes. Thus, these internal parametrizations should be the focus of future studies to improve the models.

For the Danube catchment representing a more continental climate, problems in the regional climate simulations are mainly induced by two different reasons. For ARPEGE and CHRM, the problems are related to deficiencies in the land surface parametrizations, while for HIRHAM, HadRM3H and REMO systematic errors in the dynamics appear to be causing the main errors in the simulations. The prominent summer drying problem is a major feature of all models except ARPEGE. As the summer drying problem seems to be related to the dynamics in several models it might be that deficient features in the dynamic part of CHRM and ARPEGE may also exist which are only overlaid by the systematic errors in the surface parametrizations of these two models. This should be investigated when the surface parametrizations of both models are revised.

As far as ARPEGE is concerned, the main characteristic of its systematic error is the too large snow accumulation in winter. It results in a too large runoff in spring associated with too cold spring and autumn temperatures. However, the model is not excessively cold or wet in winter (at least in the two basins). Thus, the error comes from the snow parametrization which is too snow-conservative by maintaining high albedo and weak conductivity. In earlier versions of the model, the snow cover was underestimated over Europe and the recent modifications of the scheme have led to the opposite defect. The snow-albedo feedback is very sensitive and small changes produce large effects. The underestimated snowpack of HIRHAM and REMO over the Danube catchment is probably linked to too warm temperatures in the winter. A deeper analysis of this problem is beyond our scope and is subject to future studies.

For CHRM, the major source for its summer drying problem seems to be the force-restore soil model which simulates a too weak diurnal cycle that may be also shifted in time. It also cannot retain sufficient memory of the summer heat storage which may lead to the winter cold bias. Further tests with a more advanced SVATS, coupled to a multi-level diffusive soil model, capable of retaining long term soil heat history, will be performed to address this issue.

For HIRHAM, HadRM3H, and REMO, the summer drying problem is induced by problems in the general circulation of the models where too little moisture is advected into the region (or too much divergence occurs, respectively). This leads to a lack in cloud cover which influences the surface energy fluxes. This dynamical problem of erroneous moisture transports is a large-scale problem that seems to be independent of the domain size. This is supported by REMO simulations conducted with a larger regional model domain where the summer drying problem is intensified in strength and

areal extension. This indicates that the flow through the lateral boundaries is not the main the problem. It even seems that the perfect boundary conditions may help to limit the problem for REMO. On the other hand, simulations for all RCMs (except ARPEGE) driven by GCM simulations at the lateral boundary do not show a significantly different behaviour of the summer drying problem than in the simulations considered in this study. Also previous studies (see Sect. 1) have indicated that the summer drying problem could not be explained by systematic errors in the large-scale general circulation, which forces the RCMs at the lateral boundary.

The analysis of HadRM3H was extended by comparing model convergence with that estimated directly from ERA data. The resulting convergence bias estimate *CD* was similar in behaviour to those derived using the HIRHAM and ERA indirect estimates but generally larger. This provided additional evidence for the nature of the HadRM3H biases but also that some of the hydrological cycle bias estimates could be unrealistic if there were large errors in the simulation of the underlying processes. In this instance, an early depletion of summer soil moisture indicated unrealistically small changes in soil water storage leading to unrealistically low estimates of evapotranspiration biases (and, as result, convergence biases).

As it is assumed that the erroneous moisture transports seen in HIRHAM, HadRM3H and REMO are caused by errors in the general circulation of the atmosphere, in spite of ERA boundary conditions used, it is important to find the reason for these errors. In particular it may be that these errors will be larger in real climate simulations with boundary conditions from GCM simulations instead of reanalyses (see e.g. MERCURE 2002). A more precise estimation of the causes of the errors revealed in the present studies may be carried out by systematic initial tendency error (SITE) estimates (Machenhauer and Kirchner 2000) using ERA data or the new 40 year ECMWF re-analysis data (ERA40) that are currently under production. SITE estimates can be used to assess errors in the model physics or to find missing external forcings. Alternatively, a more in depth analysis of the hydrological cycle over the region may help to isolate the precise causes of the error from the feedbacks which help to maintain it. In the present study we came closer to an understanding of the long lasting summer drying problem in regional climate simulations over Europe. However, we still do not fully understand it, and we have not managed to eliminate it completely. Further studies along the lines suggested should provide a complete understanding of the error and indicate model improvements required to remove it in future model configurations.

Acknowledgements We would like to thank Michael Botzet and Ralf Podzun from the MPI in Hamburg, Jens H. Christensen and Jan-Peter Schulz from the DMI in Copenhagen, David Hassell and Ruth Taylor from the Hadley Centre in Bracknell for their close cooperation within the MERCURE project which has been the basis of the results presented in this study. This work was sup-

ported by funding from the European Union within the MERCURE (Modelling European Regional Climate: Understanding and Reducing Errors) project (contract No. ENV4-CT97-0485).

Appendix 1

Derivation of observational estimates

First, the derivation of estimates of “observed” total runoff from the observed discharge is described. The idea behind this method is to establish a statistical relation (Eq. (5)) between model-computed monthly ensemble mean values of total runoff within a specific catchment (here the Danube and the Baltic Sea catchments) and model-computed monthly ensemble mean values of discharge from that catchment based on the HIRHAM model simulation and the hydrological discharge (HD) model (Hagemann and Dümenil 1999). Having established such a relation it is then used to obtain corresponding quasi-observed values of runoff from observed values of discharge. The HD model separates the lateral water flow into the three flow processes of overland flow, base flow, and river flow. Overland flow uses surface runoff as input, baseflow is fed by drainage from the soil and the inflow from other grid boxes contributes to riverflow. The sum of the three flow processes is equal to the total outflow from a grid box. As a general strategy, the HD model computes daily discharge at a latitude-longitude grid with 0.5° resolution. The model input fields of runoff and drainage resulting from the various (global or regional) general circulation model resolutions are therefore interpolated to the same 0.5° grid. In this study, the runoff and drainage fields of the HIRHAM simulation (see Sect. 2.1) were used to obtain the simulated discharge.

For a certain catchment, we assume that the relation between runoff R and discharge D can be approximated by Eq. (5) where L is an average lag time between R and D and the factor a is approximating a smoothing with time.

$$D(t) = a(t) \cdot R(t - L) \quad (5)$$

Optimum values of L and a_i were determined for each of the 12 calendar months from the 15 year time series of monthly total runoff and discharge values using a least square fit, allowing for integer lag values only. For the Danube catchment as well as for the Baltic Sea catchment, an optimum lag value $L = 1$ month was found. Thus, Eq. (5) becomes

$$D_i = a_i \cdot R_{i-1} \quad (6)$$

for month i . The a_i for both catchments are shown in Table 7. Assuming that Eq. (6) with the model determined a_i is valid also for observed values of discharge and runoff a set of 12 quasi-observed runoff ensemble mean values, R_{obs} , can be estimated from the observed long term mean discharge values available. Note that the long term annual means of D and R are equal.

Next, the estimation of the “observed” monthly storage changes ΔWS is described. Here, a similar statistical method was chosen as for the runoff. As these storage changes largely depend on the precipitation we approximate this relation by

$$\Delta WS_i = b_i \cdot P_i \quad (7)$$

Here, again we determine the coefficients b_i for each of the 12 calendar months from the 15 years-time series of monthly ΔWS and P of the corresponding RCM, e.g. the HIRHAM model, by a least square method. In order to obtain quasi-observed ΔWS values, ΔWS_{obs} , from observed P values the model determined relation between ΔWS and P is assumed to be valid also in reality. Using Eq. (7), we can then estimate the ΔWS_{obs} from the CRU precipitation data, P_{obs} . In this way, a quasi-observed evapotranspiration E_{obs} was estimated by inserting P_{obs} , R_{obs} and ΔWS_{obs} into Eq. (1). The so determined observed and quasi-observed values were finally used to determine biases for each model simulation.

Considering Eqs. (7) and (1) indicates that one component of the estimated evaporation is the estimated change in observed water store which, for month i is written $b_i \cdot P_i$ from Eq. (7). Now in the case of the model from which the b_i is estimated either underestimating snow-pack (observed in many of the models) or soil moisture (associated with the summer warm and dry bias seen in many of the models), if this is substantially less than underestimates of precipitation then the b_i will be too small. This implies that the estimated evaporation will also be too small and thus negative biases in evaporation underestimated.

References

- BALTEX (1995) Baltic sea experiment, BALTEX. Initial implementation plan. International BALTEX Secretariat. Publ 2, Geesthacht, Germany
- Bengtsson L (2001) Numerical modelling of the energy and water cycle of the Baltic Sea. *Meteorol Atmos Phys* 77: 9–17
- Bougeault P (1985) A simple parametrization of the large-scale effects of cumulus convection. *Mon Weather Rev* 113: 2108–2121
- Christensen JH, Christensen OB, Lopez P, van Meijgaard E, Botzet M (1996) The HIRHAM 4 regional atmospheric climate model. Danish Meteorological Institute, Sci Rep 96–4. (Available from DMI, Lyngbyvej 100, DK-2100 Copenhagen Ø, Denmark)

Table 7 Optimum values of a_i for month i obtained from Eq. (6)

| Catchment | January | February | March | April | May | June | July | August | September | October | November | December |
|------------|---------|----------|-------|-------|------|------|------|--------|-----------|---------|----------|----------|
| Danube | 0.83 | 1.04 | 0.93 | 0.81 | 0.94 | 0.95 | 1.05 | 1.22 | 2.09 | 2.54 | 1.23 | 0.97 |
| Baltic Sea | 1.10 | 1.08 | 1.00 | 0.83 | 0.59 | 0.79 | 2.11 | 2.19 | 1.93 | 1.09 | 0.83 | 1.01 |

- Christensen OB, Christensen JH, Machenhauer B, Botzet M (1998) Very high-resolution regional climate simulations over Scandinavia - present climate. *J Clim* 11: 3204–3229
- Christensen JH, Christensen OB, Schulz J-P, Hagemann S, Botzet M (2001) High resolution physiographic data set for HIRHAM 4: An application to 50 km horizontal resolution domain covering Europe. Danish Meteorological Institute, Techn Rep 01-15 4. (Available from DMI, Lyngbyvej 100, DK-2100 Copenhagen Ø, Denmark)
- Cox PM, Betts RA, Bunton CB, Essery RLH, Rowntree PR, Smith J (1999) The impact of new land surface physics on the GCM simulation of climate and climate sensitivity. *Clim Dyn* 15: 183–203
- Davies HC (1976) A lateral boundary formulation for multi-level prediction models. *Q J R Meteorol Soc* 102: 405–418
- Déqué M, Marquet P, Jones RG (1998) Simulation of climate change over Europe using a global variable resolution general climate model. *Clim Dyn* 14: 173–189
- Dickinson RE (1984) Modeling evapotranspiration for the three-dimensional global climate models. In: Hansons JE, Takahashi T (eds) *Climate processes and climate sensitivity*, Am Geophys Union, Washington, DC, pp 58–72
- Douville H, Planton S, Royer JF, Stephenson DB, Tyteca S, Kergoat L, Lafont S, Betts RA (2000) The importance of vegetation feedbacks in doubled-CO₂ time-slice experiments. *J Geophys Res* 105: 14,841–14,861
- Dümenil L, Todini E (1992) A rainfall-runoff scheme for use in the Hamburg climate model. In: Kane JP (ed) *Advances in theoretical hydrology - a tribute to James Dooge*. Elsevier Science Publishers Amsterdam pp 129–157
- Edwards J M, Slingo A (1996) Studies with a flexible new radiation code. I: Choosing a configuration for a large-scale model. *Q J Roy Meteorol Soc* 122: 689–720
- Foster DJ, Davy RD (1988) Global snow depth climatology. USAFETAC/TN-88/006, Scott Air Force Base, Ill, USA
- Frei C, Christensen JH, Déqué M, Jacob D, Jones R, Vidale PL (2003) Daily precipitation statistics in regional climate models: evaluation and intercomparison for the European Alps. *J Geophys Res* 108(D3), 4124, doi:10.1029/2002JD002287
- Gibson JK, Källberg P, Uppala S, Hernandez A, Nomura A, Serrano E (1997) Era description. ECMWF Re-Anal Proj Rep Ser 1, Reading, UK
- Giorgetta M, Wild M (1995) The water vapour continuum and its representation in ECHAM4. Max-Planck-Institute for Meteorology Rep 162 Hamburg, Germany
- Gregory D, Rowntree P R (1990) A mass-flux convection scheme with representation of cloud ensemble characteristics and stability dependent closure. *Mon Weather Rev* 118: 1483–1506
- Gregory D, Allen S (1991) The effect of convective downdraughts upon NWP and climate simulations. In: Ninth conference on numerical weather prediction, Denver, Colorado USA, pp 122–123
- Hagemann S (2002) An improved land surface parameter dataset for global and regional climate models. Max-Planck-Institute for Meteorology Rep 336, Hamburg, Germany. (Report available electronically from: http://www.mpimet.mpg.de/en/web/science/a_reports.php)
- Hagemann S, Dümenil L (1999) Application of a global discharge model to atmospheric model simulations in the BALTEX Region. *Nordic Hydrol* 30: 209–230
- Hagemann S, Dümenil L (2001) Validation of the hydrological cycle of ECMWF and NCEP reanalyses using the MPI hydrological discharge model. *J Geophys Res* 106: 1503–1510
- Hagemann S, Botzet M, Dümenil L, Machenhauer B (1999) Derivation of global GCM boundary conditions from 1 km land use satellite data. Max-Planck-Institute for Meteorology Rep 289, Hamburg, Germany. (Report available electronically from: http://www.mpimet.mpg.de/en/web/science/a_reports_archive.php?actual=1999)
- Hagemann S, Botzet M, Machenhauer B (2001) The summer drying problem over south-eastern Europe: Sensitivity of the limited area model HIRHAM4 to improvements in physical parametrization and resolution. *Physics and Chemistry of the Earth, Part B*, 26: 391–396
- Hagemann S, Machenhauer B, Christensen OB, Déqué M, Jacob D, Jones R, Vidale PL (2002) Intercomparison of water and energy budgets simulated by regional climate models applied over Europe. Max-Planck-Institute for Meteorology Rep 338, Hamburg, Germany. (Report available electronically from: http://www.mpimet.mpg.de/en/web/science/a_reports.php)
- Hulme M, Conway D, Jones PD, Jiang T, Barrow EM, Turney C (1995) Construction of a 1961–1990 European climatology for climate change modelling and impact applications. *Int J Climat* 15: 1333–1363
- Jacob D (2001) A note to the simulation of the annual and inter-annual variability of the water budget over the Baltic Sea drainage basin. *Meteorol Atmos Phys* 77: 61–73
- Jacobsen I, Heise E (1982) A new economic method for the computation of the surface temperature in numerical models. *Beitr Phys Atmos* 55: 128–141
- Jones RG, Murphy JM, Noguer M (1995) Simulation of climate change over Europe using a nested regional climate model. I: assessment of control climate, including sensitivity to location of lateral boundaries. *Q J R Meteorol Soc* 121: 1413–1449
- Källén E (1996) HIRLAM documentation manual, system 2.5. Swedish Meteorological and Hydrological Institute, pp 126 (Available from SMHI, S-60176, Norrköping, Sweden)
- Kessler E (1969) On the distribution and continuity of water substance in atmospheric circulation models. *Meteorological Monographs* 10, Am Meteorol Soc Boston, MA, USA
- Lin Y-L, Farley RD, Orville HD (1983) Bulk parametrization of the snow field in a cloud model. *J Clim Appl Meteorol* 22: 1065–1092
- Lüthi D, Cress A, Davies HC, Frei C, Schär C (1996) Interannual variability and regional climate simulations. *Theor Appl Climatol* 53: 185–209
- Machenhauer B, Kirchner I (2000) Diagnosis of systematic initial tendency errors in the ECHAM AGCM using slow normal mode data assimilation of ECMWF reanalysis data: CLIVAR Exchanges 5 (4): 9–10
- Machenhauer B, Windelband M, Botzet M, Jones RG, Déqué M (1996) Validation of present-day regional climate simulations over Europe: nested LAM and variable resolution global model simulations with observed or mixed layer ocean boundary conditions. Max-Planck-Institute for Meteorology Rep 191, Hamburg, Germany
- Machenhauer B, Windelband M, Botzet M, Christensen JH, Déqué M, Jones RG, Ruti PM, Visconti G (1998) Validation and analysis of regional present-day climate and climate change simulations over Europe. Max-Planck-Institute for Meteorology Rep 275, Hamburg, Germany
- Majewski D, Schrodin R (1994) Short description of the Europa-Modell (EM) and Deutschland-Modell (DM) of the DWD. *Quarterly Bull* (April)
- MERCURE (2002) MERCURE - Final project report, Ed.: Jones RG and Co-Workers, EU, Brussels, Belgium
- Morcrette J-J (1989) Description of the radiation scheme in the ECMWF model. ECMWF Technical Memorandum 165, Reading, UK
- Morcrette J-J (1990) Impact of changes to the radiation transfer parametrizations plus cloud optical properties in the ECMWF model. *Mon Weather Rev* 118: 847–873
- Morcrette J-J (1991) Radiation and cloud radiative properties in the ECMWF forecasting system. *J Geophys Res* 96: 9121–9132
- Nordeng T-E (1994) Extended versions of the conservative parametrization scheme at ECMWF and their impact on the mean and transient activity of the model in the tropics. ECMWF Technical Memorandum 206, Reading, UK
- Pope VD, Gallani M, Rowntree PR, Stratton RA (2000) The impact of new physical parametrizations in the Hadley Centre climate model - HadAM3. *Clim Dyn* 16: 123–146
- Ricard JL, Royer JF (1993) A statistical cloud scheme for use in an AGCM. *Ann Geophysicae* 11: 1095–1115

- Ritter B, Geleyn JF (1992) A comprehensive radiation scheme for numerical weather prediction models with potential applications in climate simulations. *Mon Weather Rev* 120: 303–325
- Roeckner E, Arpe K, Bengtsson L, Christoph M, Claussen M, Dümenil L, Esch M, Giorgetta M, Schlese U and Schulzweida U (1996) The atmospheric general circulation model ECHAM-4: model description and simulation of present-day climate. Max-Planck-Institute for Meteorology Rep 218, Hamburg, Germany
- Rubel F, Hantel M (2001) BALTEX 1/6-degree daily precipitation climatology 1996–1998. *Meteorol Atmos Phys* 77: 155–166
- Sellers PJ, Los SO, Tucker CJ, Justice CO, Dazlich DA, Collatz GJ, Randall DA (1994) A global 1 by 1 degree NDVI data set for climate studies. Part 2: the generation of global fields of terrestrial biophysical parameters from the NDVI. *Int J Remote Sens* 15(17): 3519–3545
- Slingo JM (1987) The development and verification of a cloud prediction scheme for the ECMWF model. *Q J R Meteorol Soc* 116: 435–460
- SMHI (2001) <http://www.smhi.se/sgn0102/bhdc/bhdc.htm>
- Smith RNB (1990) A scheme for predicting layer clouds and their water content in a general circulation model. *Q J R Meteorol Soc* 116: 435–460
- Smith TM, Reynolds RW, Livezey RE, Stokes D.C (1996) Reconstruction of historical sea surface temperatures using empirical orthogonal functions. *J Clim* 9: 1403–1420
- Sundqvist H (1978) A parametrization scheme for non-convective condensation including prediction of cloud water content. *Q J R Meteorol Soc* 104: 677–690
- Sundqvist H (1988) Parametrization of condensation and associated clouds for weather prediction and general circulation simulations. In: Schlesinger ME (ed) *Physically based modeling and simulation of climate and climate change*. Dordrecht, NL, Reidel, pp 433–461
- Tiedtke M (1989) A comprehensive mass flux scheme for cumulus parametrization in large-scale models. *Mon Weather Rev* 117: 1779–1800
- Viterbo P, Beljaars ACM (1995) An improved land-surface parametrization in the ECMWF model and its validation. *J Clim* 8: 2716–2748
- Vidale PL, Lüthi D, Frei C, Seneviratne S, Schär C (2003) Predictability and uncertainty in a regional climate model. *J Geophys Res*, 108(D18), 4586, doi:10.1029/2002JD002810
- Wild M, Ohmura A, Gilgen H, Roeckner E (1995) Validation of GCM simulated radiative fluxes using surface observations. *J Clim* 8: 1309–1324
- Wild MA, Dümenil L, Schulz J-P (1996) Regional climate simulation with a high resolution GCM: surface hydrology. *Clim Dyn* 12: 755–774
- WMO (World Meteorological Organization) (1988) Concept of the global energy and water cycle experiment. Tech Rep WCRP-5, WMO/TD 215, Geneva, Switzerland
- Xu K-M, Randall D (1996) A semiempirical cloudiness parametrization of ruse in climate models. *J Atmos Sci* 53: 3084–3102